Nerve Growth Cone Lamellipodia Contain Two Populations of Actin Filaments That Differ in Organization and Polarity

Annette K. Lewis and Paul C. Bridgman

Department of Anatomy and Neurobiology, Washington University School of Medicine, St. Louis, Missouri 63110

Abstract. The organization and polarity of actin filaments in neuronal growth cones was studied with negative stain and freeze-etch EM using a permeabilization protocol that caused little detectable change in morphology when cultured nerve growth cones were observed by video-enhanced differential interference contrast microscopy. The lamellipodial actin cytoskeleton was composed of two distinct subpopulations: a population of 40–100-nm-wide filament bundles radiated from the leading edge, and a second population of branching short filaments filled the volume between the dorsal and ventral membrane surfaces. Together, the two populations formed the three-dimensional structural network seen within expanding lamellipodia. Interaction of the actin filaments with the ventral membrane surface occurred along the length of the filaments via membrane associated proteins. The long bundled filament population was primarily involved in these interactions. The filament tips of either population appeared to interact with the membrane only at the leading edge; this interaction was mediated by a globular Triton-insoluble material.

Actin filament polarity was determined by decoration with myosin S1 or heavy meromyosin. Previous reports have suggested that the polarity of the actin filaments in motile cells is uniform, with the barbed ends toward the leading edge. We observed that the actin filament polarity within growth cone lamellipodia is not uniform; although the predominant orientation was with the barbed end toward the leading edge (47–56%), 22–25% of the filaments had the opposite orientation with their pointed ends toward the leading edge, and 19–31% ran parallel to the leading edge. The two actin filament populations display distinct polarity profiles: the longer filaments appear to be oriented predominantly with their barbed ends toward the leading edge, whereas the short filaments appear to be randomly oriented.

The different length, organization and polarity of the two filament populations suggest that they differ in stability and function. The population of bundled long filaments, which appeared to be more ventrally located and in contact with membrane proteins, may be more stable than the population of short branched filaments. The location, organization, and polarity of the long bundled filaments suggest that they may be necessary for the expansion of lamellipodia and for the production of tension mediated by receptors to substrate adhesion molecules.

During development, neuronal growth cones respond to environmental cues by regulating the rate and direction of neurite outgrowth. Although several cytosolic processes are intermediate in these responses, the mechanical events underlying motility are effected by the cytoskeleton. Several mechanical events are clearly involved, including extension of lamellipodia and filopodia, retrograde translocation of actin filaments, and production of tension through interaction with the substratum. Each of these phenomena potentially result from the polymerization of actin filaments or the interactions between actin and myosins (40). Despite an abundance of evidence linking the actin cytoskeleton with motility and locomotion, both the complexity of the actin meshwork and the difficulty in preserving this complexity have frustrated previous efforts to accurately describe mechanical events at the molecular level.

While a significant effort has been made to determine the organization of the actin cytoskeleton in motile cells (3, 16, 17, 23, 24, 36, 41, 44, 45), there is still controversy about which of the several different preparations used to visualize the cytoskeleton produce faithful representations of the filament organization. The central problem is that actin filaments are labile and subject to distortion during processing for electron microscope visualization. Of the many different methods, two techniques, negative staining and freeze-etch rotary shadowing, present the fewest technical limitations. Samples prepared using either of these methods appear to have the least distortion of the filament network (16, 36). However, these two procedures have not provided concordant views of the actin cytoskeleton. The filaments in negatively stained samples have generally appeared relatively long and straight, extending from the leading edge toward

the central region, with minimal interaction between filaments (36). In freeze-etched samples, filaments at the leading edge have appeared shorter, often bending and branching, forming a complex three-dimensional interwoven network (16). In addition, both techniques have required removal of the plasma membrane to varying degrees which restricts the ability to study the interaction between the filaments and the membrane. Such interaction may be important because of the potential role of actin filaments in producing tension by binding to intramembrane proteins that act as receptors for substrate molecules (27).

The actin cytoskeleton of nerve growth cones has not been extensively studied using negative stain (19), or at all using freeze etching. Studies have been done using thin section electron microscopy (30, 45) and more recently using extracted whole mount cytoskeletons (24); details of the growth cone actin filament organization have remained relatively obscure using these techniques. For instance, in the latter study, Letourneau compared the actin organization in growth cones and neurites and found that removal of the plasma membrane by Triton extraction before fixation resulted in retention of an actin network in growth cones but not in neurites. However, it has been shown in fibroblasts that Triton extraction before fixation results in a significant loss of actin filaments (35), suggesting that this was also the case in the growth cones. In the same study (24), fixation before Triton extraction resulted in a microtrabecular lattice-like appearance (44). This lattice has been shown to result from artifacts caused by a combination of osmium tetroxide postfixation, dehydration, and critical point drying of samples for electron microscopy (7, 26, 32, 37). Our attempts to circumvent the artifacts described above using rapid freezing and freeze substitution to prepare whole mounts or thin sections of growth cones were largely successful (3, 11). However, a precise picture of the actin organization was hindered by the fact that individual filaments are difficult to see clearly against the background of cytoplasmic globular proteins present in unextracted cells. In addition, even when critical point drying is done with great care, as in our previous studies (3, 11), it can lead to slight distortion (7).

To understand the dynamics of cell motility it is necessary to unambiguously determine the polarity of the actin filaments in the leading edge of motile cells. The discovery of myosin I and its likely role in cell motility (29), in addition to recent work showing that the direction of movement of actin along myosin molecules is determined entirely by the polarity of actin filaments (34), stress the need to accurately determine actin filament polarity. The polarity of actin filaments can be visualized by decorating the filaments with either myosin S1 fragment (S1) or heavy meromyosin (HMM)[1] (18, 28). The S1 and HMM form arrowheads along actin filaments, the barb of the arrowhead corresponding to the plus or rapidly polymerizing end, and the point to the minus or slowly polymerizing end. A number of studies have been done using various motile cell types to determine the polarity of actin filaments in the cytoskeleton (1, 17, 19, 33, 36). In general, the results have suggested that all actin filaments have the same orientation, with their barbed ends toward the leading edge (1, 19, 36). The organization of the actin filaments within lamellipodia is complex and the assumption that all filaments are oriented with their barbed ends directed towards the leading edge of the cell would appear to be an oversimplification of the actual organization. In addition, the polarity of actin filaments in growth cones of primary neurons has not been previously determined.

We now further investigate growth cone actin filament organization and polarity in permeabilized growth cones using procedures to minimize the distortion and loss of actin filaments that can accompany permeabilization and combine this with negative staining and deep freeze etching. The results show that the actin cytoskeleton in the peripheral region of the growth cone is made up of two distinct populations of actin filaments. In addition, contrary to previous reports from other cell types (1, 17, 19, 33, 36), we observed that actin filaments within the thinly spread lamellipodia of growth cones did not have uniform polarity. The two populations which differ in organization and orientation with respect to polarity can be distinguished in both the negatively stained and freeze-etched images. In addition, we investigated the interaction of the actin filaments with the membrane surface. These results suggest that the assumption that actin filaments of peripheral lamellipodia are made up of a single population with a uniform polarity is not well founded, and models based upon this assumption may have to be modified to take into account a more complex actin filament organization.

Materials and Methods

Superior Cervical Ganglia Dissection and Explant Culture

Superior cervical ganglia (SCG) were dissected from embryonic day 20–21 rat pups, desheathed, and cut into approximately eight explants (20). Explants were maneuvered onto either 25-mm-round glass coverslips coated with 1 mg/ml polyornithine (Sigma Chemical Co., St. Louis, MO) and 16 μg/ml laminin (Collaborative Research, Waltham, MA), 3-mm-round glass coverslips coated with laminin, or 600 mesh gold electron microscope grids supporting a laminin-treated 1% formvar film. Cultures were grown for 15–20 h at 37°C in C10-2 culture media: MEM (Gibco Laboratories, Grand Island, NY) with 10% horse serum (Gibco Laboratories), 2% embryo extract (Gibco Laboratories), 0.6% glucose, 1.4 mM L-glutamine (Gibco Laboratories), and nerve growth factor (~25 biological U/ml) (20).

Light Microscope Observation during Saponin or Triton Perfusion

Cultures grown on 25-mm-round glass coverslips were mounted into a Dvorak-Stotler chamber in Hepes C10-2 media (bicarbonate replaced by 25 mM Hepes, pH 7.3) (Irvine Scientific, Santa Ana, CA) and put onto a 37°C microscope stage. Warmed solution containing either 0.02% saponin (Sigma Chemical Co.) or 0.05% Triton X-100 (Pierce Chemical Co., Rockford, IL), and 8×10^{-8} M phalloidin (Sigma Chemical Co.) in PHEM buffer (60 mM Pipes [Sigma Chemical Co.], 25 mM Hepes, 10 mM EGTA, 2 mM $MgCl_2$, pH 6.9) was perfused through the chamber via gravitational flow. Based on the flow rate and tubing volume we could calculate the arrival time of the detergent containing solution. Because the flow was nonlaminar, some mixing at the front could occur, potentially resulting in an initial detergent gradient. Observations were made with differential interference contrast optics using a 63×, 1.4 NA objective and a matched condenser. Video rate background subtraction and contrast enhancement was done as previously described (11).

Saponin Permeabilization

0.02% saponin and 8×10^{-8} M phalloidin in PHEM buffer was warmed

1. *Abbreviations used in this paper*: HMM, heavy meromyosin; SCG, superior cervical ganglia; VEC-DIC, video-enhanced differential interference microscopy.

to 37°C and applied to the cultures grown on gold grids for 10 min. Cultures were then rinsed with PHEM buffer, fixed for 10 min with 1% glutaraldehyde (Polysciences Inc., Warrington, PA) in PHEM buffer, and negatively stained. We tested whether the addition of phalloidin during the permeabilization affected the filaments by comparing negatively stained samples permeabilized in the presence or absence of phalloidin. We observed no obvious differences between the two conditions.

Filipin Permeabilization

4% filipin (Polysciences Inc.) in DMSO was diluted into 8×10^{-8} M phalloidin in PHEM buffer to a final concentration of 0.04% (4), warmed to 37°C, and applied to the cultures grown on gold grids for 15 min. Cultures were rinsed with PHEM buffer, fixed for 10 min with 1% glutaraldehyde in PHEM buffer, and negatively stained.

Triton Extraction

Saponin-permeabilized and fixed cultures were rinsed in PHEM buffer, treated for 10 min with 0.05% Triton X-100, and negatively stained or frozen.

Physically Sheared Samples for Freeze Etching

Cultures grown on 3-mm glass coverslips were prepared in two different ways. After saponin permeabilization samples were fixed in 0.25% glutaraldehyde in PHEM buffer. They were then treated with 0.2% tannic acid (Fischer Scientific, Fair Lawn, NJ) in KM buffer (70 mM KCl, 5 mM $MgCl_2$) for 30 min, followed by 1% uranyl acetate (Electron Microscopy Sciences, Ft. Washington, PA) in KM buffer for 30 min. After a rinse in distilled water, a second piece of coverglass was applied on top of the sample. The two coverglasses with the sample sandwiched between were then pressed together with forceps, moved in a roughly circular pattern relative to each other, and immediately frozen as a unit.

The second procedure was modified from Heuser and Anderson (15). Cultures were transferred to a low calcium Hepes-buffered defined composition culture medium (modified from Bottenstein and Sato [2]; Joklik MEM was substituted for Dulbecco's MEM, and EGTA was added to adjust the calcium concentration to ~100 nM [9]). Either poly L-lysine or polyornithine were then added at a concentration of 0.3 mg/ml. After 20–30 s the samples were transferred to PHEM buffer diluted 1:2 with distilled water for ~15 s. They were then transferred to a shallow beaker containing 0.1% glutaraldehyde in PHEM buffer and sonicated for 15–20 s using a probe sonicator with a 1/8-inch tip operating at a power output of ~5 W and 23 KHz. Samples were further fixed with 1% glutaraldehyde for 10 min, rinsed in distilled water and then frozen.

Preparation of HMM and S1

Rabbit skeletal muscle myosin was prepared following the method of Kielley and Harrington (21). HMM and myosin S1 fragment (S1) were prepared following the method from Margossian and Lowey (25). In brief, for HMM, rabbit skeletal muscle myosin was digested with 0.05% trypsin (Sigma Chemical Co.) for 2 min. The digestion was stopped by addition of 0.3% soybean trypsin inhibitor (Sigma Chemical Co.). The digested myosin was dialyzed overnight in 0.02 M KCl, 0.01 M KH_2PO_4, pH 6.5, and 0.001 M DTT, and centrifuged 60 min at 28,000 rpm (50 Ti rotor; Beckman Instruments, Inc., Fullerton, CA) to separate the HMM from undigested myosin and light meromyosin. For S1, myosin was digested with 0.03 mg/ml papain for 3 min. The digestion was stopped by addition of 0.001 M iodoacetic acid. The digested myosin was then centrifuged 90 min at 30,000 rpm and dialyzed overnight in 0.05 M Tris-Cl pH 8, 0.001 M DTT, and 0.002 M $MgCl_2$.

Preparation of Decorated Samples for Negative Stain

0.25 mg/ml HMM or myosin S1, 0.02% saponin (Sigma Chemical Co., St. Louis, MO) and 8×10^{-8} M phalloidin (Sigma Chemical Co.) in PHEM buffer (60 mM Pipes [Sigma Chemical Co.], 25 mM Hepes (Irvine Scientific), 10 mM EGTA, 2 mM $MgCl_2$, pH 6.9) was warmed to 37°C and applied to the cultures grown on gold grids for 5–30 min. Cultures were then rinsed with PHEM buffer, fixed and extracted with 1% glutaraldehyde (Polysciences Inc.) and 0.2% Triton X-100 (Pierce Chemical Co.) in PHEM buffer for 30–60 min, and negatively stained.

Preparation of Decorated Samples for Freeze Etching

0.02% saponin and 8×10^{-8} M phalloidin in PHEM buffer was warmed to 37°C and applied to the cultures grown on 3-mm glass coverslips for 5 min followed by a 10-min incubation in 0.5 mg/ml myosin S1. Cultures were rinsed with PHEM buffer, fixed for 10 min in 1% glutaraldehyde in PHEM buffer, rinsed, and extracted for 10 min with 0.5% Triton in PHEM buffer. Samples were then rinsed with KM solution (70 mM KCl, 5 mM $MgCl_2$), incubated for 1 h in 0.2% tannic acid in KM solution, rinsed with KM solution, and incubated for 1 h in 1% uranyl acetate in KM solution (14), and then frozen.

Negative Staining

Samples were rinsed in distilled deionized water and passed through four drops of 40 μg/ml bacitracin (Sigma Chemical Co.), lightly blotted, passed through four drops of 3% phosphotungstic acid (Sigma Chemical Co.), pH 7, blotted, and put in an 80°C oven to dry for 2 min. Samples were photographed using a JEOL 1200EX or 100CX electron microscope at 80 or 100 KV.

Freezing

After rinsing in distilled water, samples were frozen in a stirred mixture of propane and ethane (3:1) cooled with liquid nitrogen. Rapid entry into the freezing mixture was provided by a spring driven device (5).

Freeze Etching and Rotary Shadowing

Samples were placed on the precooled stage of a Balzer's 400D freeze-etch device. The stage was warmed to between −102 and −95°C and the samples were etched under high vacuum (2×10^{-6} Torr) for 1–3 h. The stage temperature was then lowered to −120°C and the samples were shadowed at an angle of 20° with ~1.2 nm of metal using a pellet composed of platinum, rhenium, and iridium, followed by a thicker carbon layer (90° angle) (6). The average thickness of the metal and carbon layers were estimated from quartz crystal monitor readings. The temperature was calibrated using a thermocouple connected directly to the surface of the sample holder.

Replicas were warmed to room temperature, removed from the glass with 3% hydrofluoric acid, washed with two changes of water, and picked up on uncoated 600 mesh EM grids. Replicas were photographed at 100 KV using a JEOL 1200 EX. Images of replicas were photographically reversed so that metal grains appeared white.

Determination of Polarity

Photographs of samples with overall distinct decoration were analyzed to quantify the different filament orientations. In these samples the location of the leading edge was determined relative to the area being analyzed, and considered as the hypotenuse of a 90° angle. All filaments that ran perpendicular to this line, plus or minus 45°, were considered to be oriented either toward or away from the leading edge, depending on the arrowhead direction, and all filaments that ran parallel to the line, plus or minus 45°, were classed as parallel to the leading edge. All filaments on which the decoration could be clearly seen were counted and this number was divided by the total number of filaments in the field to determine the percent of total filaments with distinct polarity. The percentage of the filaments with different orientations were then determined within this population of filaments. Sample size for quantitation was six fields for negative stain samples and 12 fields for freeze-etch samples. Filament polarity in the freeze-etch samples was determined by a naive observer.

Results

Permeabilization of Growth Cones

It was necessary to develop a method of growth cone permeabilization that extracted soluble cytoplasmic proteins but did not cause the extensive retraction or detachment of the growth cone often observed with conventional detergent permeabilization. Although inclusion of fixative in the permeabilization solution can alleviate retraction and detachment, one of our goals was to develop a system for labeling actin

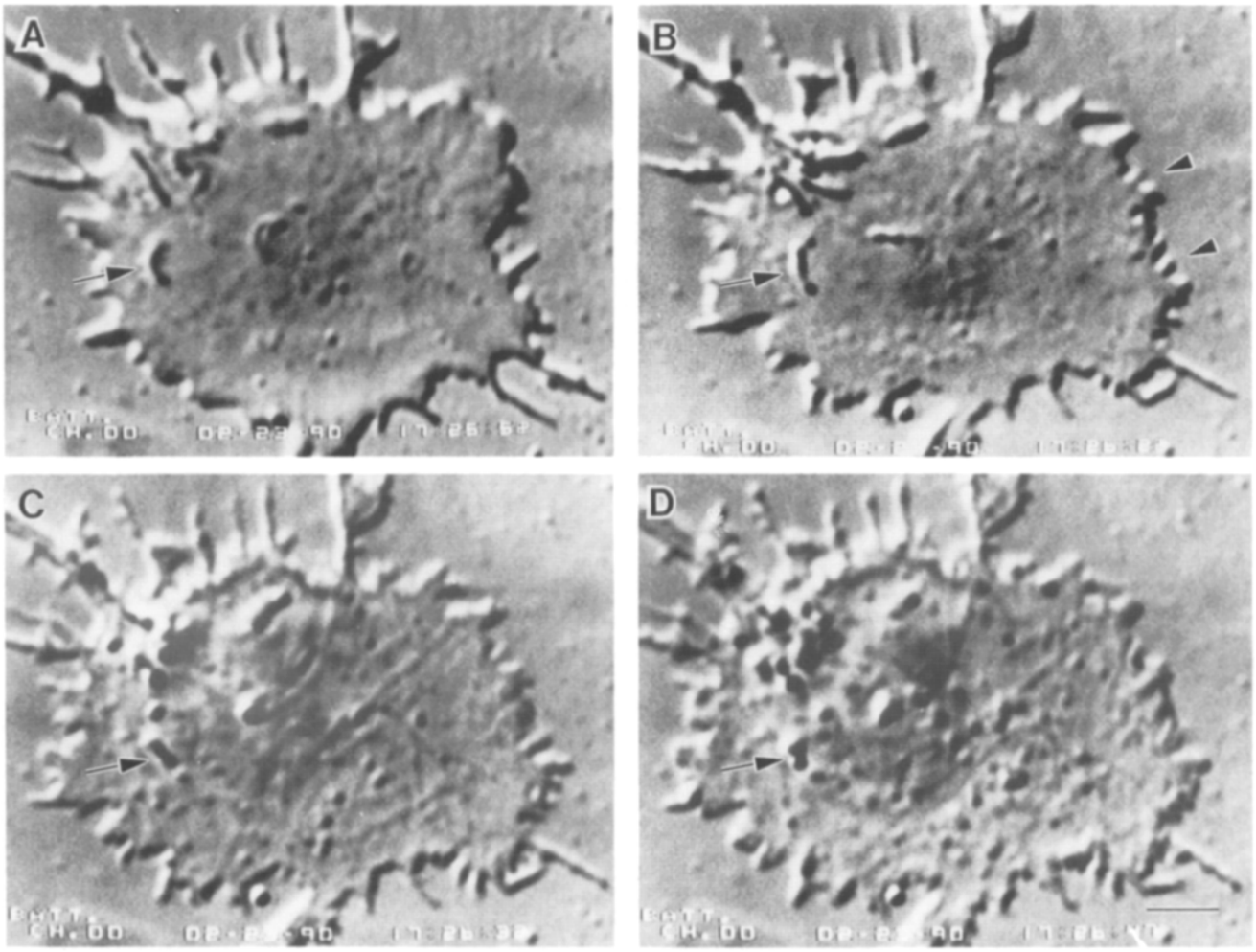

Figure 1. A growth cone observed with VEC-DIC microscopy during perfusion with the saponin permeabilization solution. (*A*) Growth cone just before the beginning of perfusion. Lamellipodial region continues to be active showing both protrusion and retraction of both leading edge and filopodia. Mitochondria appear normal (*arrow*). (*B*) 20 s after the beginning of perfusion note fine scalloping of a portion of the leading edge (*arrowheads*). (*C*) Upon arrival of the detergent front at the growth cone the membrane collapses onto the cytoskeleton making the filamentous structures more apparent. Mitochondria begin to vesiculate (*arrow*). (*D*) Completely permeabilized growth cone; there were no observable changes with continued perfusion. Bar, 2 μm.

with myosin S1, heavy meromyosin, or antibodies, which precluded the addition of fixative. We therefore refined the permeabilization conditions of living cultures to prevent detergent-induced morphological change. Preliminary experiments with a variety of detergents or membrane permeabilizing agents indicated that saponin, Triton, or the polyene antibiotic, filipin, were good potential candidates. A series of experiments were done using video-enhanced differential interference contrast (VEC-DIC) microscopy to monitor growth cone morphology during permeabilization with either saponin or Triton X-100. After identifying active, advancing growth cones, we initiated perfusion of calcium free buffer (PHEM) containing 8×10^{-8} M phalloidin, and either 0.02% saponin or 0.5% Triton X-100 (Fig. 1).

Cells perfused with the saponin solution showed only very subtle morphological change, suggesting that the saponin treatment had little effect on the cytoskeleton or general morphology of the cell. ~40 s elapsed between initiation of perfusion (Fig. 1 *A*) and the arrival of the detergent front at the sample (Fig. 1 *C*); during this time the lamellar region continued to be active. Just before (~10 s) the calculated arrival of the saponin front there was an increase in Brownian motion of small organelles within the central region of the growth cone. This was probably due to the arrival of the PHEM buffer and perhaps a low concentration of saponin resulting from mixing caused by the nonlaminar flow. Control perfusion experiments with the PHEM buffer also resulted in an increase in Brownian motion. In the saponin-treated samples there was a barely detectable lamellar retraction, giving the appearance of a slight increase in the length of filopodia and sometimes a fine scalloping of the marginal edge (Fig. 1 *B*). This retraction appeared to relax to varying degrees during permeabilization (see Fig. 2 *C*). When the saponin front arrived, a fast wave of permeabilization passed over the cell, seen as collapse of the membrane onto the cytoskeleton (filamentous structures were now more apparent) (Fig. 1 *C*). Membrane vesicles also became more prominent and mitochondria appeared to vesiculate. The cell was completely permeabilized (Fig. 1 *D*) within 2–4 s after the initial collapse and the permeabilized growth

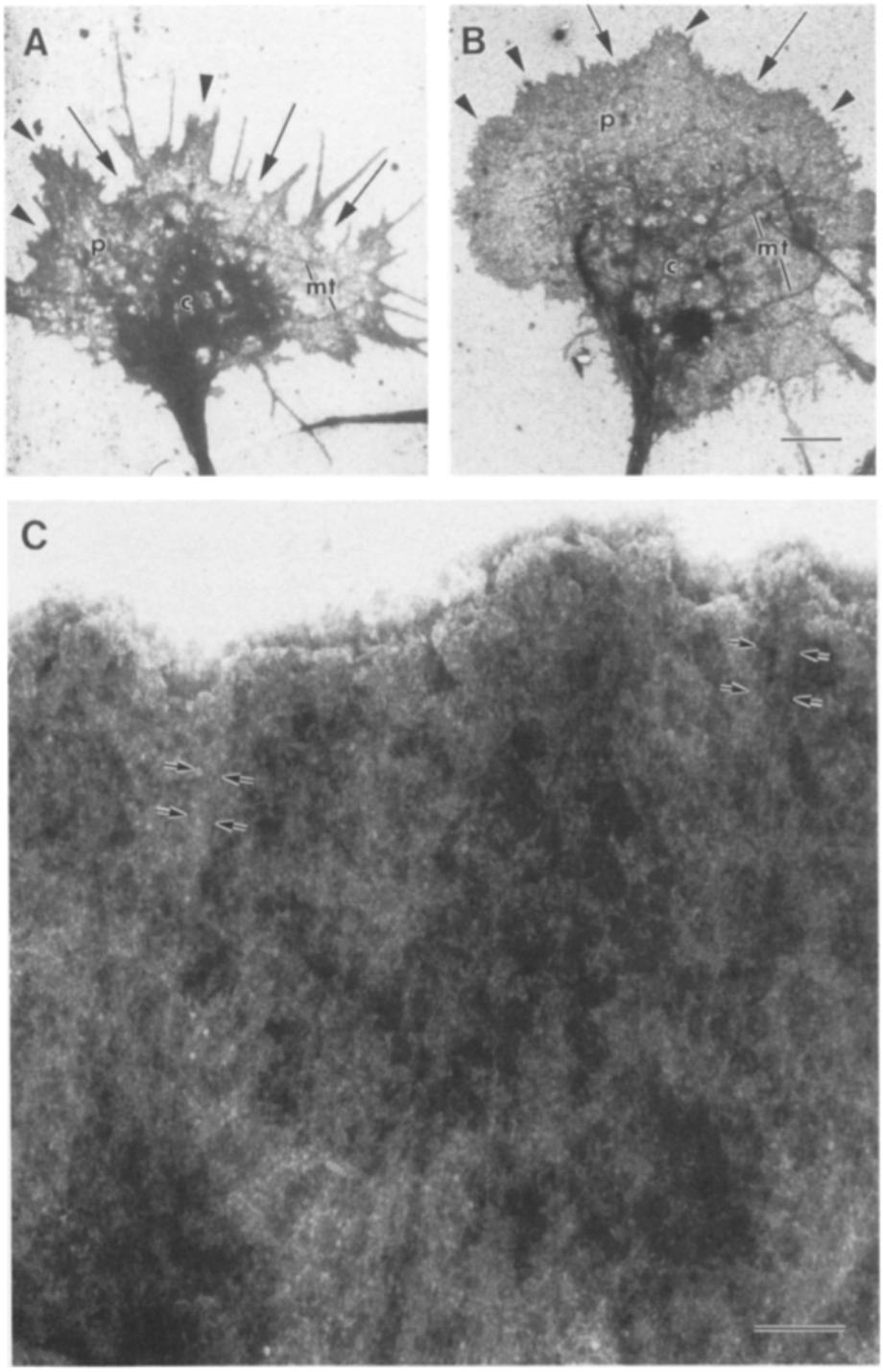

Figure 2. Growth cones prepared by saponin permeabilization, fixation, and negative stain. (*A* and *B*) Low magnification views of two growth cones that are filopodial (*A*) or lamellipodial (*B*) in appearance. Both images were obtained in low magnification mode without an objective aperture. Areas can be classified as protrusive (*arrowheads*) and retractive (*arrows*) in both types of growth cones based upon criteria established from VEC-DIC observations of living growth cones. Microtubules (*mt*) can be seen extending occasionally into the peripheral region of the growth cones. Peripheral (*p*) and central (*c*) domains can be distinguished in both low and higher magnification views. (*C*) Higher magnification view (normal imaging mode with objective aperture) showing the relatively high electron density of a thinly spread lamellipodia. At this magnification individual filaments cannot be seen but a faint indication of bundles (*small arrows*) radiating from the leading edge can be detected. The leading edge membrane appears relatively smooth indicating that the permeabilization protocol had little affect on the growth cone morphology. Bars: (*A* and *B*) 3 μm; (*C*) 0.2 μm.

cones were observed for up to 5 min with no further detectable changes. Addition of rhodamine phalloidin to the perfusion medium resulted in labeling of actin filaments within seconds of permeabilization and was useful for qualitative assessment of the amount of actin filament retention (data not shown). No detectable loss of rhodamine phalloidin staining was seen with continued perfusion of the saponin solution.

Perfusion of living cells with the Triton solution resulted in a considerably more abrupt permeabilization (data not shown). Again, there was an initial increase in Brownian motion of small organelles, but in contrast to the saponin permeabilization, these small organelles were often seen to move from the central region into the thin peripheral region, effectively filling the growth cone. With the arrival of the main Triton front the membrane immediately dissolved (within one to three video frames). This was apparent from an abrupt change in contrast and texture of the growth cone image. The shadow cast outline of the growth cone was not easy to distinguish from the background after the membrane was dissolved with Triton. This made it somewhat difficult to determine to what extent the overall morphology had been affected by the Triton extraction. Sometimes it appeared that patches of the cytoskeleton were removed with the mem-

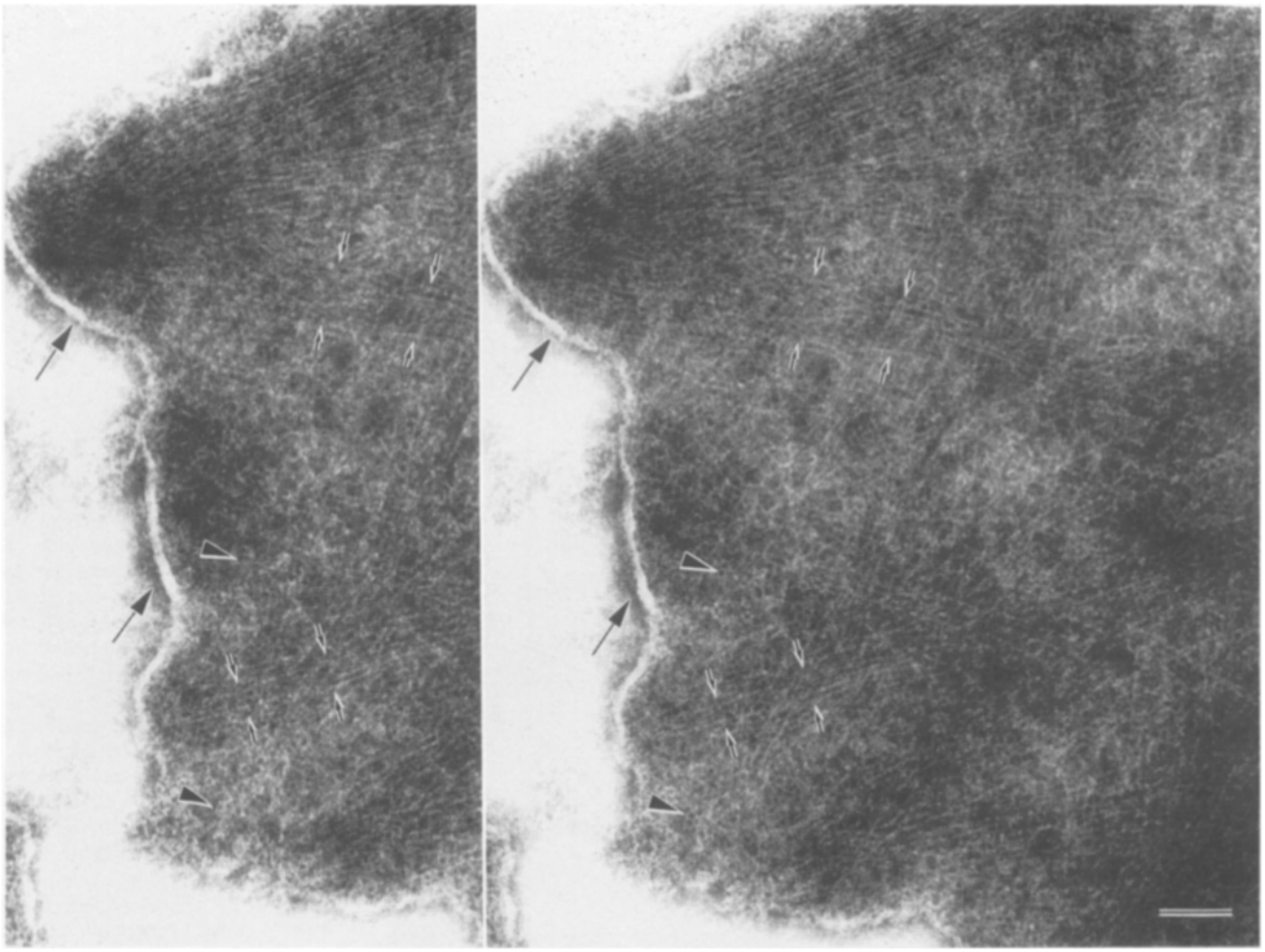

Figure 3. Stereo view of the actin filament organization in a thin lamellipodia from a growth cone that was saponin permeabilized, fixed and then negatively stained. 5–10-nm holes that were produced by the saponin can be seen in the membrane (*arrowheads*). When seen on edge the membrane at the leading margin appears white (*large arrows*). Although less obvious at this relatively high magnification, actin filament bundles containing 6–12 filaments radiate from the leading margin membrane (*small arrows* delineate representative bundles). A meshwork of shorter filaments is also present throughout the lamellipodia; the orientation of filaments is random and fills the volume between the dorsal and ventral membrane surfaces. Bar, 0.1 μm.

brane and often, over the course of 5 min postperfusion, more areas of the cytoskeleton were slowly swept away by the continued flow of the perfusion solution. This reduced the cytoskeleton to a patchwork of individual filament bundles attached to the substrate, rather than a distinct growth cone as seen in the saponin perfusion. Occasionally the entire growth cone skeleton detached and floated away.

These data suggest that Triton treatment before fixation potentially allows for loss of some or all of the cytoskeletal elements and overall disruption of the cytoskeletal morphology. On the other hand, permeabilization with low concentrations of saponin causes little change in cytoskeletal morphology at the light microscope level. Although recordings were not obtained from growth cones permeabilized with filipin, their appearance in the light microscope after treatment was similar to that of saponin-permeabilized samples. Due to this difference between Triton and saponin or filipin treatment, most samples prepared for EM were first permeabilized with saponin, then fixed with glutaraldehyde, and depending on the experiment, the membrane was sometimes further extracted with Triton to fully expose the cytoskeleton.

Negative Stain

Low magnification views of negatively stained saponin extracted samples revealed the entire outline of the growth cone (Fig. 2). This was useful for identifying areas of the leading edge likely to have been undergoing expansion as opposed to retraction or stasis at the time of permeabilization. In VEC-DIC observations of living growth cones, expansion of lamellipodia was associated with a relatively smooth, broad protrusion with a convex shape, while retraction was associated with a more convoluted margin, often with a concave shape between protruding filopodia (see 8, 31). In addition, expanding lamellipodia often appeared to have a broader shadow cast rim in VEC-DIC suggesting that they were slightly thicker. Filopodia protruded most frequently at the leading edge and retracted most frequently at the base of the growth cone in the region closely associated with the

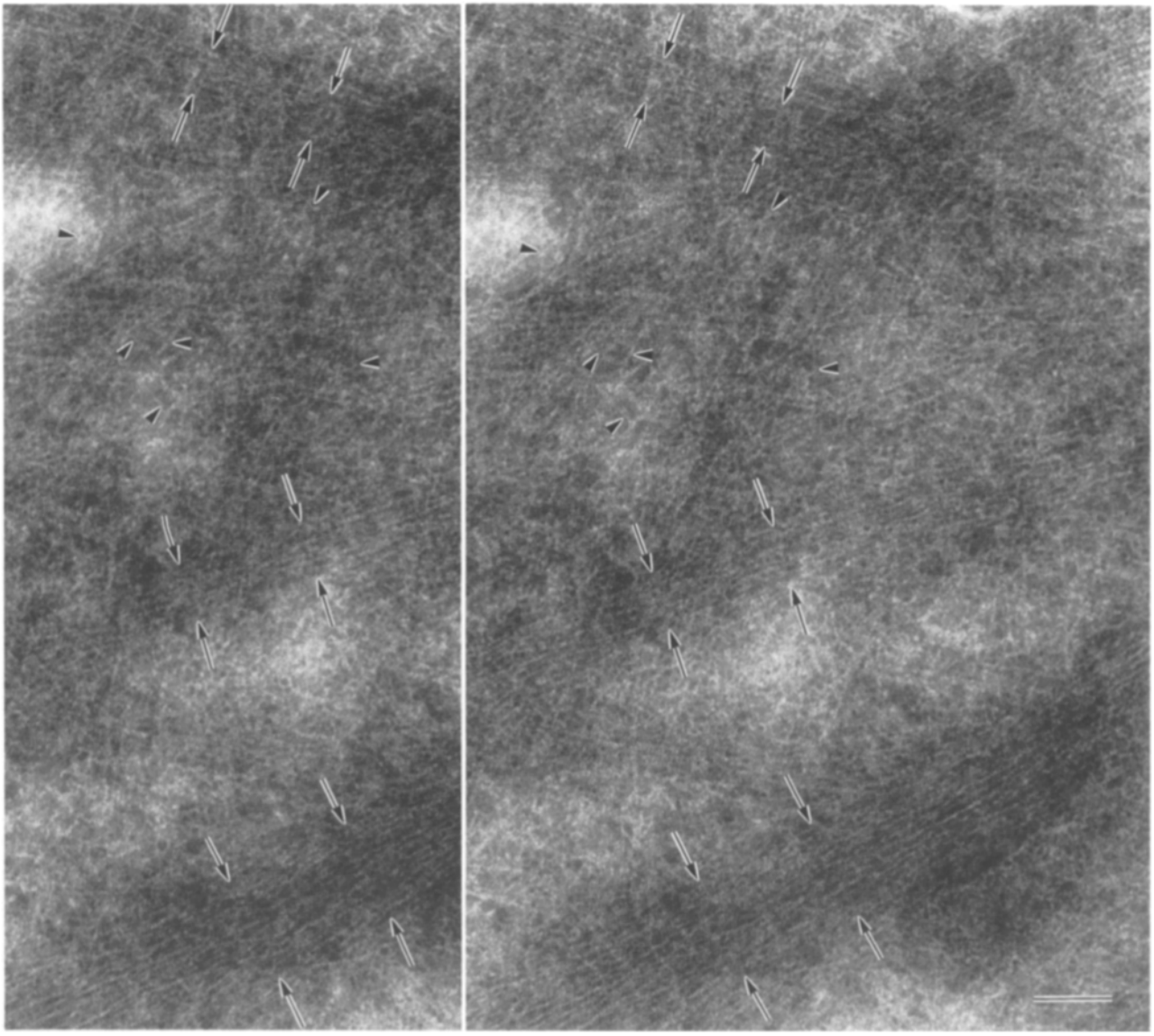

Figure 4. Stereo view of a lamellipodia further back from the leading edge. The thicker area has more volume than the thin edge seen in Fig. 3. The filaments that make up the meshwork of filaments can be more clearly seen (*arrowheads*) interspersed between filament bundles (*arrows*). Bar, 0.1 μm.

connecting neurite. When these criteria (shape and thickness) were used on the negatively stained growth cones it was often possible to find areas fitting both descriptions on individual growth cones (Fig. 2, *A* and *B*). When combined with the information on the relative position of the growth cone margin, it was possible to classify these areas as representative of the regions undergoing expansion and retraction/stasis seen in living growth cones. We classified the actin organization on this basis. Although this classification is not rigorous since we did not make light and electron microscopic observations on the same growth cones, it should represent a good approximation of the functional state at the time of permeabilization. Using this procedure we obtained several hundred images from ~50 thinly spread growth cones; the data described below is based on these images.

As noted in the perfusion experiments, the leading edge in saponin-permeabilized samples generally did not appear altered by the permeabilization (Fig. 2 *C*), although slight scalloping was occasionally seen in some regions. In addition, the peripheral and central regions of the growth cones could be clearly distinguished in both low and high magnification views. Samples that had been prepared by Triton extraction before fixation confirmed the light microscopic observations; growth cones appeared partially or fully retracted, or when not retracted had a lower filament density and contained patches devoid of any filaments.

High magnification images of negatively stained growth cones permeabilized with saponin showed some features unique to this method of preparation. First, the plasma membrane could be detected, especially when viewed at the edge of the growth cone margin (Fig. 3). The holes in the membrane, which were formed by saponin, accumulated stain and appeared as small dark disks distributed over the entire surface of the growth cone. When viewed as stereo pairs the samples showed a surprising amount of volume (Fig. 4); they showed less collapse of structure than is normally associated

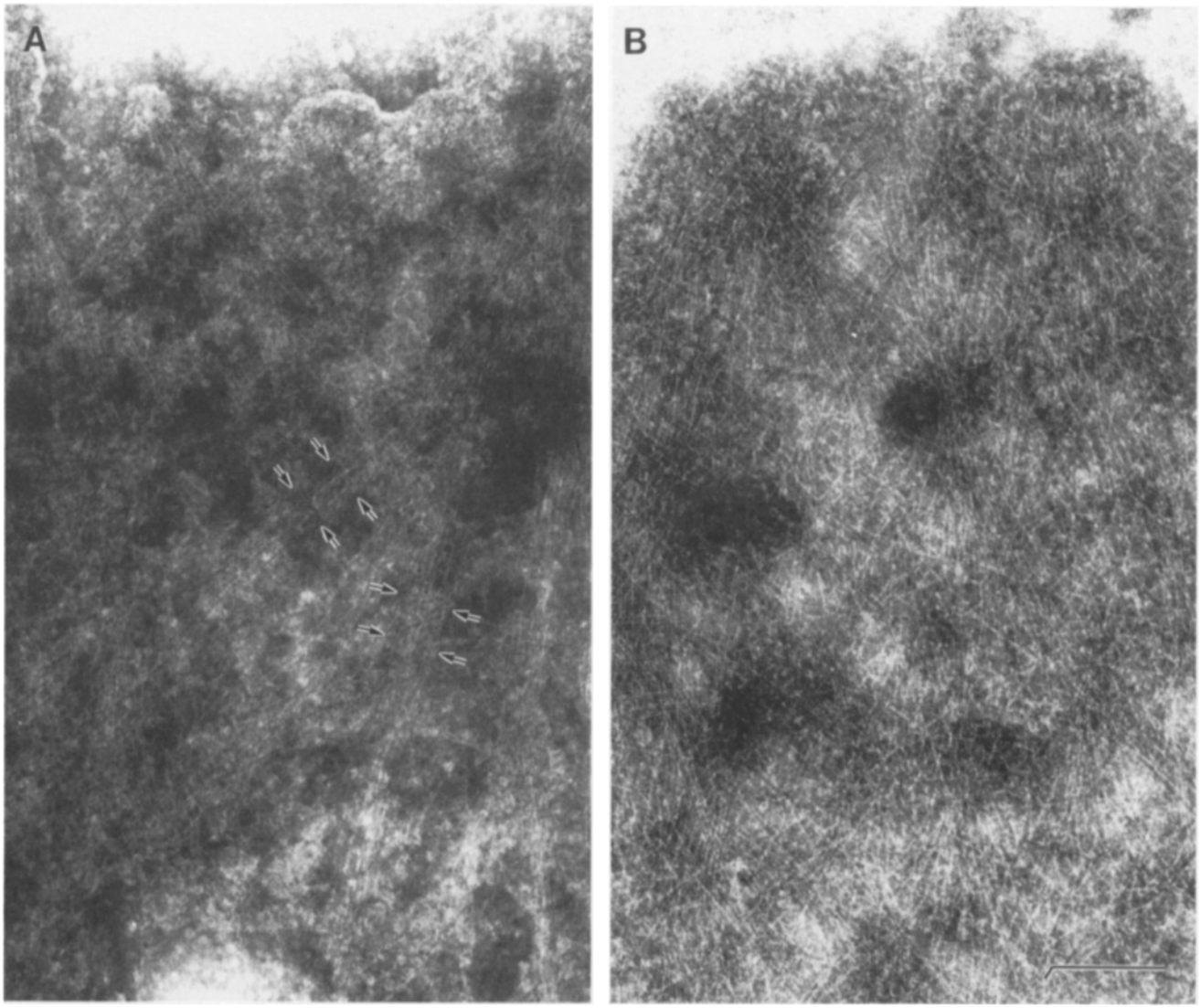

Figure 5. Triton extraction results in loss of actin filament bundles in lamellipodia. (*A*) From a growth cone that was treated with saponin, fixed, and then negatively stained. 40–100-nm-wide actin filament bundles (*small arrows*) radiate from the leading margin and traverse the length of the lamellipodia. (*B*) From a growth cone that was saponin permeabilized, fixed, and then Triton extracted before negative staining. The distinct 40–100-nm-wide filament bundles are no longer obvious. Individual filaments splay out from the leading edge; most do not appear bundled. Bar, 0.2 μm.

with negative stain specimens extracted with detergents such as Triton. Because of the increased volume, the overall electron density of the samples was high (Fig. 2 *C*) and it was necessary to use relatively high acceleration voltages (100 KV) to obtain images of reasonable quality. The high voltage requirement in turn reduced the contrast of the actin filaments. To minimize these difficulties imposed by increased sample thickness we imaged relatively thin, well spread growth cones.

Areas corresponding to regions of putative lamellipodial expansion had a very dense actin meshwork dominated by 40–100-nm-wide bundles containing 6–12 parallel filaments apparently of uniform length, radiating from the leading edge of the growth cone (Figs. 3 and 4). The bundles were relatively long (3–5 μm), frequently extending the length of the lamellipodium (3–6 μm). The proximal ends of the bundles usually terminated near the intersection with the central region of the growth cone. Because of the relatively large thickness in this region it was often difficult to clearly see the termination of the bundle but in some cases it was clear that the termination took one of two forms: either an abrupt ending of filaments or through splaying of the filaments.

Individual bundles intersected one another at oblique angles, creating the appearance of a loosely woven fabric. In regions of the lamellipodium classified as stationary or retracting the bundles did not radiate from the leading margin and were absent from the area immediately behind the marginal edge. However, because of the overlapping weave of the bundles radiating from adjacent expanding regions, the more proximal region of these areas of the lamellipodium usually did contain the bundles. Sometimes the protruding regions on either side of the putative area of retraction contained an especially high density of bundles, suggesting that they may have moved laterally during or before retraction. In stereo, images of the filaments within a single bundle appeared to be in a single plane. When two bundles appeared

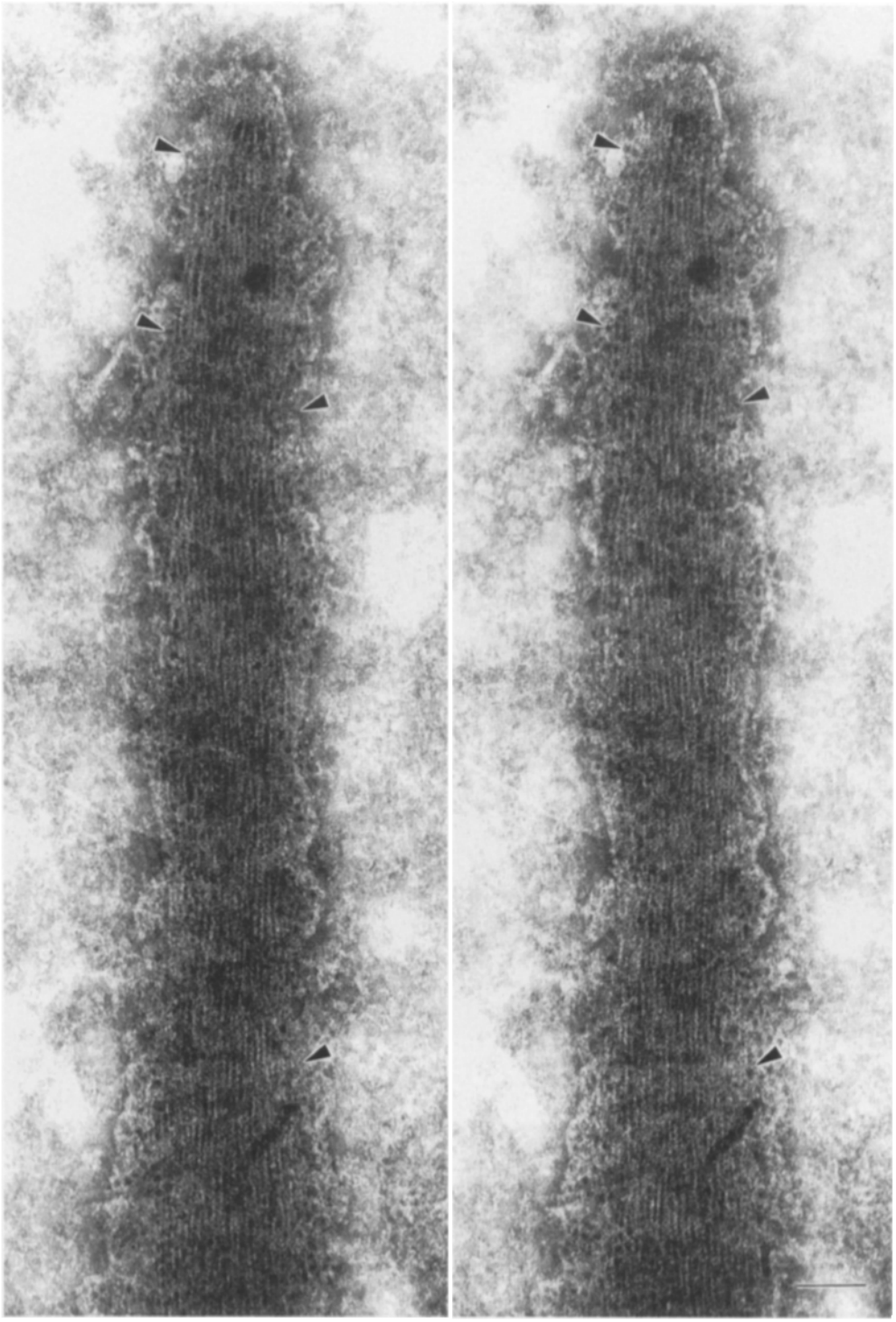

Figure 6. Stereo view of a filopodium from a growth cone that was saponin permeabilized, fixed, and then negatively stained. Filaments run parallel as a tightly packed bundle along the entire length of the filopodium. Holes in the membrane (*arrowheads*) produced by saponin are especially obvious along the edge of the filopodium. Bar, 0.06 μm.

to intersect by two-dimensional imaging, examination in stereo revealed that they passed each other in different planes, usually with no detectable interaction.

Interspersed between these bundles was a separate dense meshwork consisting of much shorter actin filaments (Figs. 3 and 4). This meshwork also extended into the areas of the growth cone classified as retracting or stationary. In stereo images it was apparent that the filaments within the meshwork appeared to be oriented randomly, branched or intersecting at oblique angles and filled the volume between the upper and lower membranes (Figs. 3 and 4). In thicker areas, such as near the intersection with the central region of the growth cone, the meshwork dominated the images, while in the thin peripheral regions the bundles were most apparent.

To determine the accuracy of the organization observed in saponin-treated samples, we compared them with filipin permeabilized samples (data not shown). In these samples, small bundles of actin filaments could be seen through the membrane extending from the leading edge. In stereo views, the bundles had the appearance of a fabric weave similar to

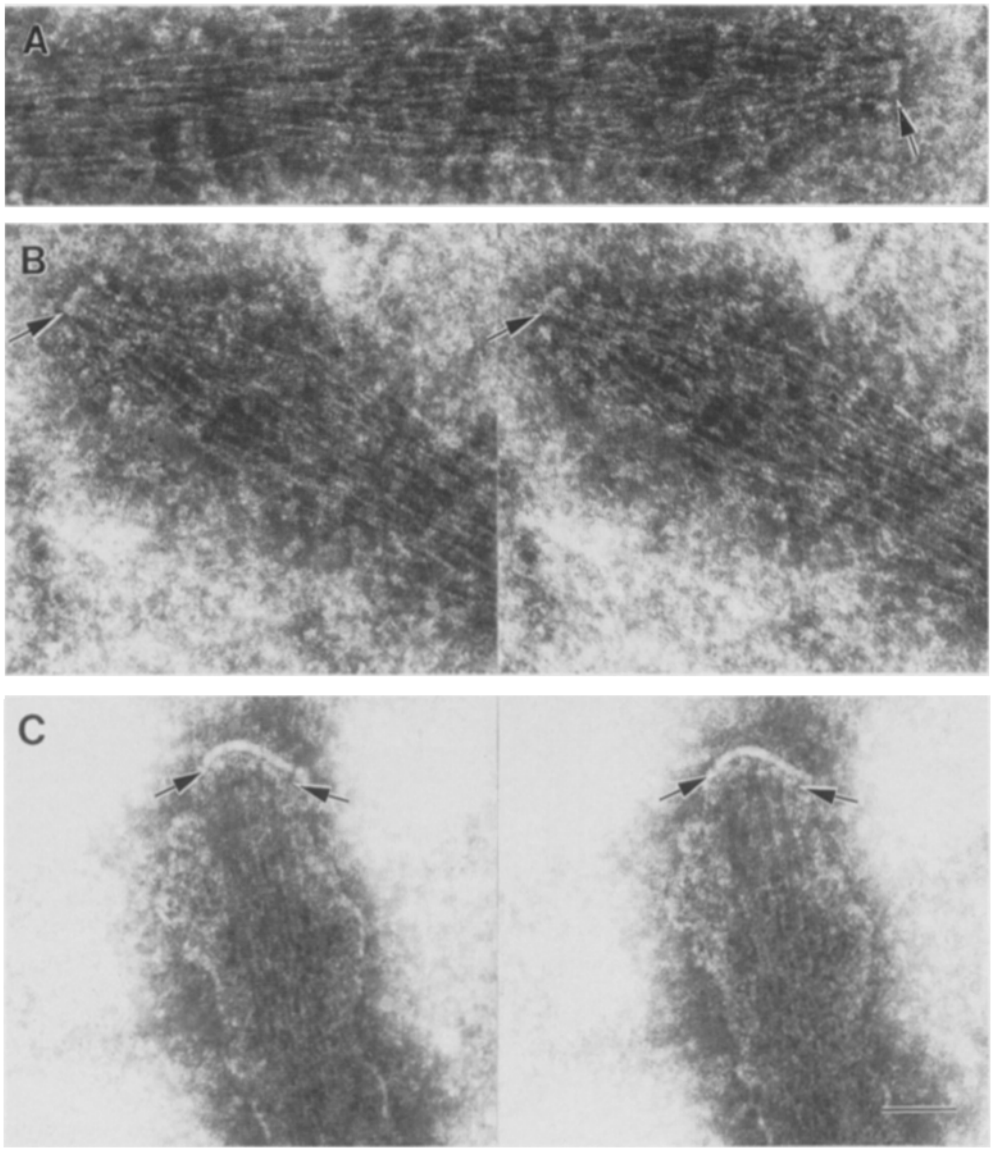

Figure 7. Effects of Triton extraction on actin filament organization of filopodia. (*A*) From a growth cone that was saponin permeabilized, fixed, and then Triton extracted before negative staining. The filament bundle remains intact but some subtle differences are detectable: gaps between filaments are slightly more prominent and filaments occasionally cross at oblique angles. A Triton-insoluble material (*arrow*) is apparent at the end of the filopodium. (*B*) A stereo view of the end of the same filopodium shown in (*A*). (*C*) From a growth cone that was saponin permeabilized, fixed and then negatively stained. A globular material possibly related to the Triton-insoluble particles seen at the filament tips in *A* and *B* can be seen (*arrows*). Bar, 0.06 μm.

the bundles observed in the saponin-treated samples. Shorter filaments, corresponding to the second filament population, were also present.

After fixation, some saponin-permeabilized samples were extracted with Triton to fully remove the membrane. This led to some noticeable differences in the appearance of the actin filament organization within lamellipodia (Fig. 5). In part, these differences resulted from the decrease in relative contrast between individual and bundled filaments; individual filaments were now more distinct. However, there were also fewer distinct bundles within the lamellipodia. Although relatively long actin filaments emerged from the leading edge and radiated towards the central region of the growth cone, they tended to splay out as a continuous sheet of filaments rather than follow a parallel course as the individual oriented bundles seen in saponin and filipin treated samples (Fig. 5 *B*). Stereo images of the Triton-extracted samples did not have as much volume as the samples only extracted with saponin (data not shown). Since there was less of a three-dimensional image, short filaments, presumably composing the meshwork population, were prominent, however, the orientation of these filaments relative to the membranes (z-axis) was not obvious.

The actin bundles forming the core of filopodia were distinct from the lamellar bundles described above. They usually contained >15 filaments and were tightly packed (60–180 nm wide). In contrast to the lamellar bundles, the filaments of filopodial bundles appeared to be in several planes, forming roughly cylindrical rather than planar bundles (Fig. 6). Filopodia could be seen around the entire periphery of some growth cones (Fig. 2 *A*), however the characteristics of the actin bundles appeared to be location specific. In the regions classified as quiescent, such as near the attachment of the neurite, the tight filopodial actin bundles often ended at the base of the filopodium. In putative active regions (towards the leading margin) the filopodial bundles continued into the lamellar region 0.5–2.0 μm, either as tightly packed filament bundles or they split apart, gaining the appearance of the lamellar bundles. We directed our attention to the organization of the actin bundles in filopodia along the leading margin. In the saponin- and filipin-treated samples the filaments in the filopodial bundles

were tightly packed and ran parallel to each other (Figs. 6 and 7 *C*). In the Triton-extracted filopodia, the filaments did not appear to be as tightly bundled and were slightly wavy, producing gaps in the bundles where the filament split into opposing waves and then rejoined again (Fig. 7, *A* and *B*). In stereo images the Triton-extracted bundles were less cylindrical than the saponin-treated samples, appearing flattened against the substratum.

In apposition with the actin filaments along the leading edge of the Triton-extracted growth cone, we observed small bits of irregularly shaped Triton-insoluble material. This material was particularly prominent at the tips of filopodia (Fig. 7, *A* and *B*). In saponin-extracted samples, we sometimes detected a globular material immediately adjacent to the cytoplasmic membrane surface, possibly the same as the Triton-insoluble material seen in the Triton-extracted samples (Fig. 7 *C*). In both cases, actin filament ends appear to directly contact this globular material.

Negative Stain of Decorated Samples

To determine the polarity of actin filaments we decorated some samples with HMM or myosin S1. Unfortunately, it was not possible to accurately determine the filament polarity when the cells were saponin permeabilized, decorated with HMM or S1, fixed, and negatively stained because the high actin filament density combined with the high density of decorating proteins resulted in an electron dense, low contrast image of the individual decorated filaments. Even if decorated samples were fixed and then Triton extracted the electron density was too high, presumably because it was difficult to fully wash out the unbound myosin fragments before fixation. An alternative protocol was therefore used for the decorated negatively stained samples: after incubation of the saponin permeabilized cells with HMM or S1, the cells were rinsed, and simultaneously fixed and Triton extracted. Using this protocol, sufficient contrast was obtained in ~30 thinly spread growth cones to determine the direction of the arrowhead formations on many of the decorated filaments. As described above, Triton extraction of the samples may cause some slight distortion of the filament organization, however, this protocol provides more accurate structural preservation than protocols used in previous studies requiring Triton or glycerol extraction before filament decoration (1, 36). In addition, using this protocol, the filament polarity could be determined throughout the length of a lamellipodia, rather than exclusively at the extreme edge.

The outline of the growth cone could easily be seen in low magnification views of decorated samples (Fig. 8 *A*). Many of the filaments appeared relatively long with the bulk of the filaments running essentially perpendicular to the leading edge. At higher magnification (Fig. 8 *B*), the details of the filament organization were distinct; actin filaments were a variety of lengths and oriented in all directions. Although all of the filaments appeared to be decorated, the direction of the arrowheads formed by the binding of HMM (or S1) to the filaments was distinguishable on approximately one third of the total filaments within a field. The inability to determine the polarity on the remaining filaments resulted from lack of sufficient contrast or overlap of filaments. From the filaments in which the polarity could clearly be seen, it was readily apparent at a qualitative level, that the polarity of the actin filaments was not uniform with all of the barbed ends toward the leading edge. Instead, a number of filaments either had their pointed ends toward the leading edge or were parallel to the leading edge. Due to the tendency of the negative stain to be significantly darker at the extreme edges of some of the samples it was often difficult to distinguish individual filaments in this area and thus the arrowhead direction (see Fig. 9 *A*). However, the filaments that could be distinguished within this region were not exclusively oriented with their barbed ends toward the leading edge.

Some simple quantitation was done using samples with clearly distinguished decoration (sample size 6). The polarity could be determined on 33% of the total filaments; of these, 56% were oriented with their barbed ends towards the leading edge, 25% had the opposite polarity with their pointed ends toward the leading edge, and 19% were parallel to the leading edge.

To determine whether there was a difference in the polarity of the actin filaments based on their location in the lamellipodia, we analyzed the polarity of filaments at the leading edge (Fig. 9 *A*), and in more proximal regions of the lamellipodia (Fig. 9 *B*). The polarity ratios from these two subgroups did not vary significantly from those calculated for the total lamellipodial region: for the peripheral region, 61% were oriented with their barbed ends towards the leading edge, 21% were pointed towards the leading edge, and 18% were parallel to the leading edge (sample size 4); for the central regions, 55% were oriented with their barbed ends towards the leading edge, 31% were pointed towards the leading edge, and 14% were parallel to the leading edge (sample size 3). These data suggest that there is no region within the lamellipodia where the filaments have uniform polarity.

The actin filament bundles forming the core of filopodia were too tightly packed to accurately distinguish the polarity of the individual filaments. However, the polarity of many of the filaments entering a filopodial bundle at its base could be distinguished; the majority of the filaments entering a bundle had their barbed ends toward the tip. Occasionally, however, filaments with their pointed ends toward the tip could be distinguished entering a filopodial bundle. It was not possible to tell whether these filaments continued all the way to the tip of the filopodia.

Freeze Etching

To verify and expand upon the observations from the negative stain samples, we looked at the actin organization in samples prepared using several different procedures before rapid freezing and deep etching. It is often not possible to see through the entire depth of the filament layer in etched, rotary shadowed samples, since only the top layer of filaments receives enough metal coating to be easily detectable. Filaments lying underneath are not coated unless the filament density is low or the upper filaments are physically removed before freezing or after freezing by knife fracturing. In addition, the overlying membrane must be removed to allow visualization of the cytoskeleton. This is in contrast to the negatively stained saponin-permeabilized samples, in which, in relatively thin areas, both membranes and the entire depth of the filament layer can be visualized, even if the filament density is high. For this reason, several different approaches were used to prepare samples for etching, with the

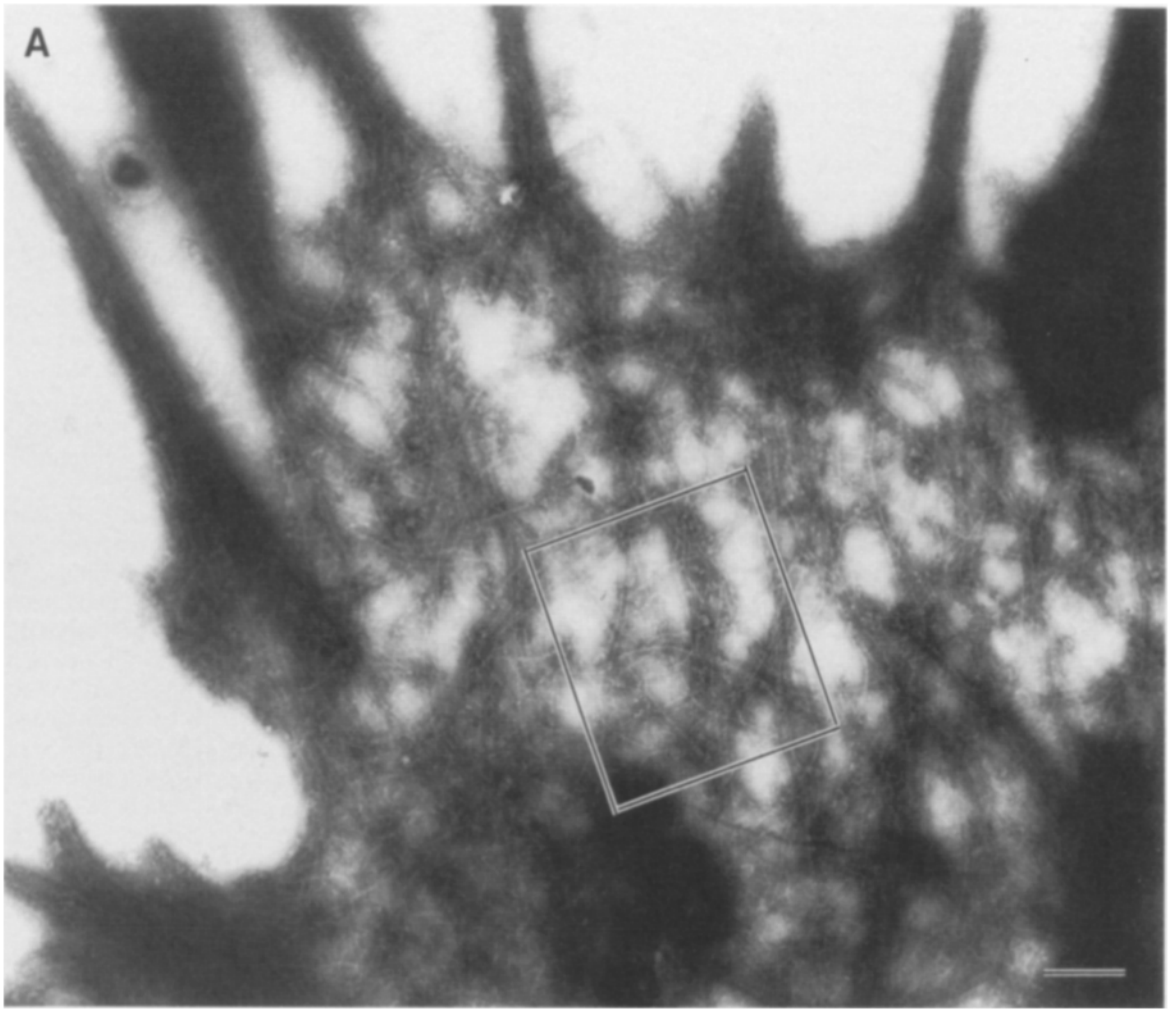

Figure 8. (*A*) Relatively low magnification image of a portion of a growth cone decorated with HMM and viewed with negative stain. The outline of the growth cone is distinct; filopodia project from the margin of this growth cone. The leading edge is toward the top of the picture. An interwoven network of filaments can be seen at this magnification. The boxed area is shown in *B*. (*B*) Higher magnification showing the decoration pattern of individual actin filaments. The polarity can be determined in approximately one third of the filaments (*arrowheads*). The actin filaments appear to be organized with a mixture of polarities. Some filaments are oriented with their barbed ends directed towards the leading edge (top of picture) while others have the opposite orientation or are roughly parallel with the edge. Bars: (*A*) 0.5 μm; (*B*) 0.1 μm.

goal of obtaining views that revealed different actin filament layers and their interaction with the ventral membrane.

Triton-Extracted Samples

The majority of the etched samples were prepared in the same manner as the Triton-extracted negative stain samples with saponin permeabilization, fixation, and Triton extraction before freezing. This allowed visualization of growth cones with their full complement of actin filaments (Fig. 10). However, there is a noticeable artifact complicating the interpretation of these freeze-etch images. The placement of a few of the surface fibers in the Triton-extracted samples was often inaccurate because they were susceptible to displacement by fluid movement before freezing. These surface fibers are prominent in the freeze etch images due to the increased contrast resulting from the large amount of metal they receive during rotary shadowing. Such filament displacement also occurs during the negative staining process of Triton-extracted samples, where an occasional filament can be seen extending out beyond the boundary of the growth cone. However, these filaments are less prominent in the negative stain images since their contrast is not enhanced relative to the main population of filaments. This artifact needs to be taken into consideration when viewing the Triton-extracted freeze etch samples.

In general, the actin organization in the Triton-extracted freeze-etched samples was similar to that seen in the Triton-extracted negatively stained samples. The filament array of the freeze-etched samples had more depth in stereo images, and filaments often appeared to be slightly more intertwined and relaxed, making sinuous bends (Figs. 10 and 11). Again, within lamellipodia there appeared to be two filament populations: a predominant population that emerged from the leading edge as a sheet of roughly parallel filaments that were occasionally bundled and, interspersed between this sheet of filaments, a meshwork of shorter, branched filaments oriented roughly parallel to the z-axis. These shorter fila-

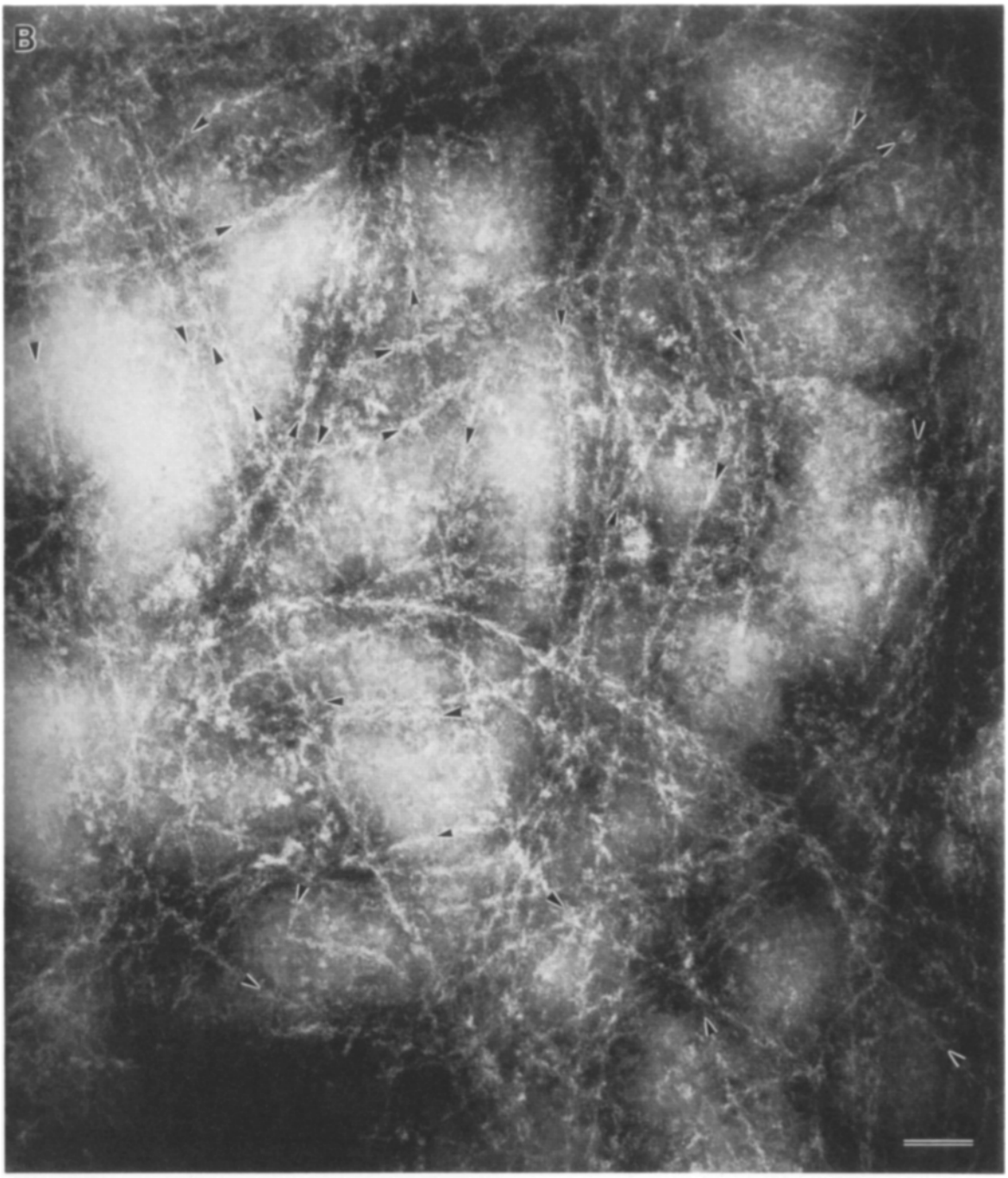

Figure 8.

ments appeared more numerous on the dorsal surface of the filament array (they appeared lighter in the images because of a thicker platinum coat), while the longer filaments radiating from the leading edge were closer to the substratum (they appeared darker). Together, the two populations produced a highly interwoven meshwork of filaments with the main axis of filament orientation forming a radial pattern that emerged from the leading edge. As in the negative stain samples, the ends of the filaments at the leading edge were associated with an irregular-shaped Triton-insoluble material (Fig. 11). Sometimes multiple filament ends appeared connected by a single globular piece of the material. Occasionally, on high magnification images, filaments with a smaller diameter than that of the actin filaments appeared to be crosslinking the directionally oriented actin filaments (Fig. 11). The identity of these filaments is unknown, however, it has been suggested by Hirokawa et al. (17) that these thin short filaments are myosin molecules crosslinking actin filaments.

Actin bundles forming the core of filopodia were also similar to those seen in the Triton-extracted negative stain samples but often appeared to be more tightly packed and cylindrical (Fig. 12). This resulted in bundles that were smaller in width (50–80 nm). The tightly packed appearance could also be a result of the increased diameter of the filaments due

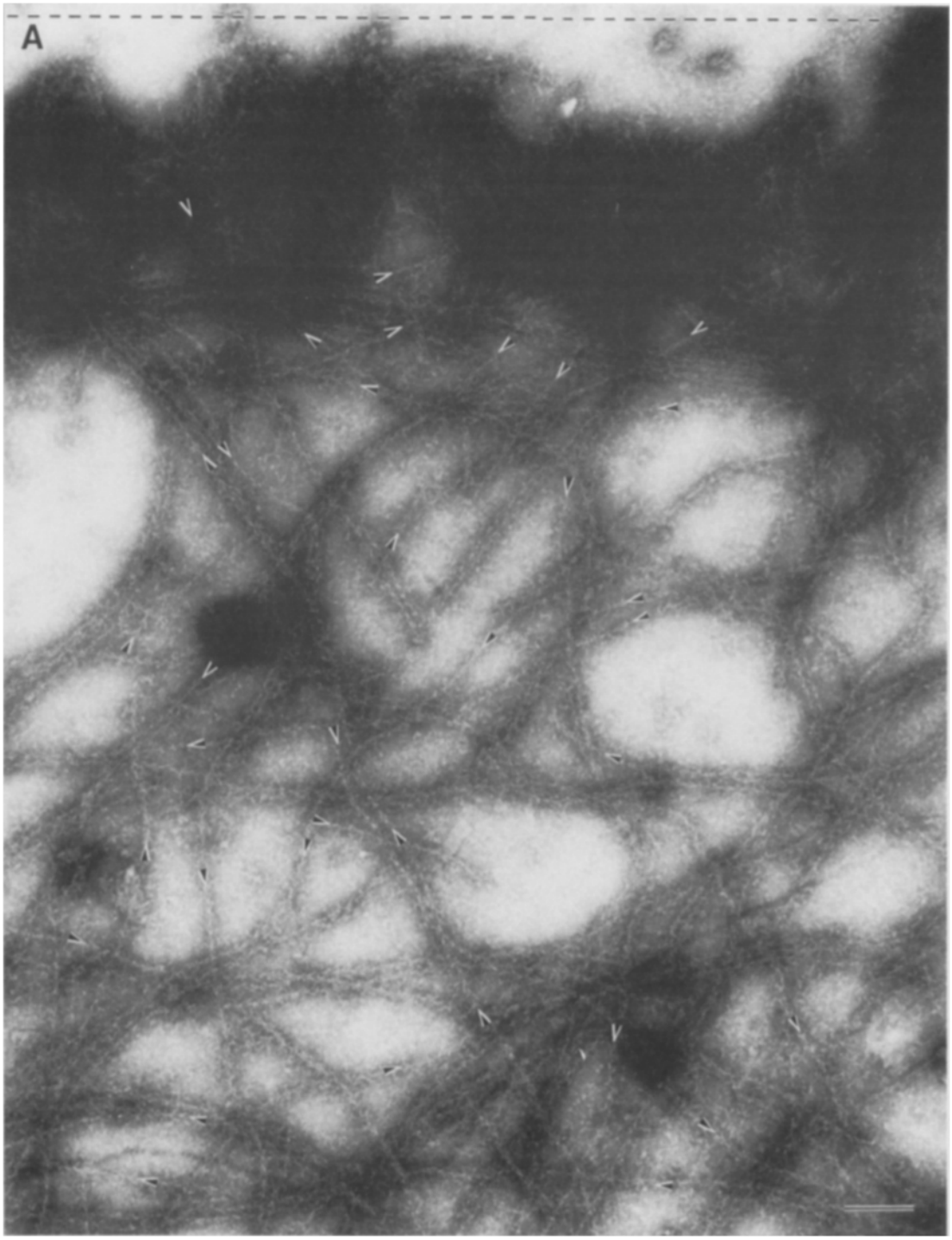

Figure 9. (*A*) High magnification view of a lamellipodial type (no filopodia) growth cone decorated with HMM. The leading edge of the growth cone is present at the top of the picture. Similar to the growth cone in Fig. 8, actin filaments show a mixture of polarities (*arrowheads*). (*B*) High magnification view from the same growth cone in *A* but further from the leading edge. Again, actin filaments show a mixture of polarities. Bars: (*A*) 0.2 μm; (*B*) 0.1 μm.

to their shadowing with a metal coat. As in the negative stain samples, an irregular shaped Triton-insoluble material was apparent at the ends of filopodia.

Physically Sheared Growth Cones

To determine the relationship between the filaments and the ventral surface of the membrane, we attempted to remove the dorsal membrane and the upper layers of actin filaments. We found that knife fracturing of rapid frozen growth cones was not useful since the fracture plane never entered the cytoplasm of the thinly spread peripheral region of the growth cones. Therefore, we resorted to physically shearing the cells before freezing. This was done in two different ways. First, saponin-permeabilized, fixed samples were sheared between two closely applied pieces of glass coverslips immediately before freezing. This resulted in removal of varying degrees of the top membrane and filaments. In favorable views, the relationship between the underlying membrane and actin filaments could be seen (Fig. 13). Again, filaments in lamel-

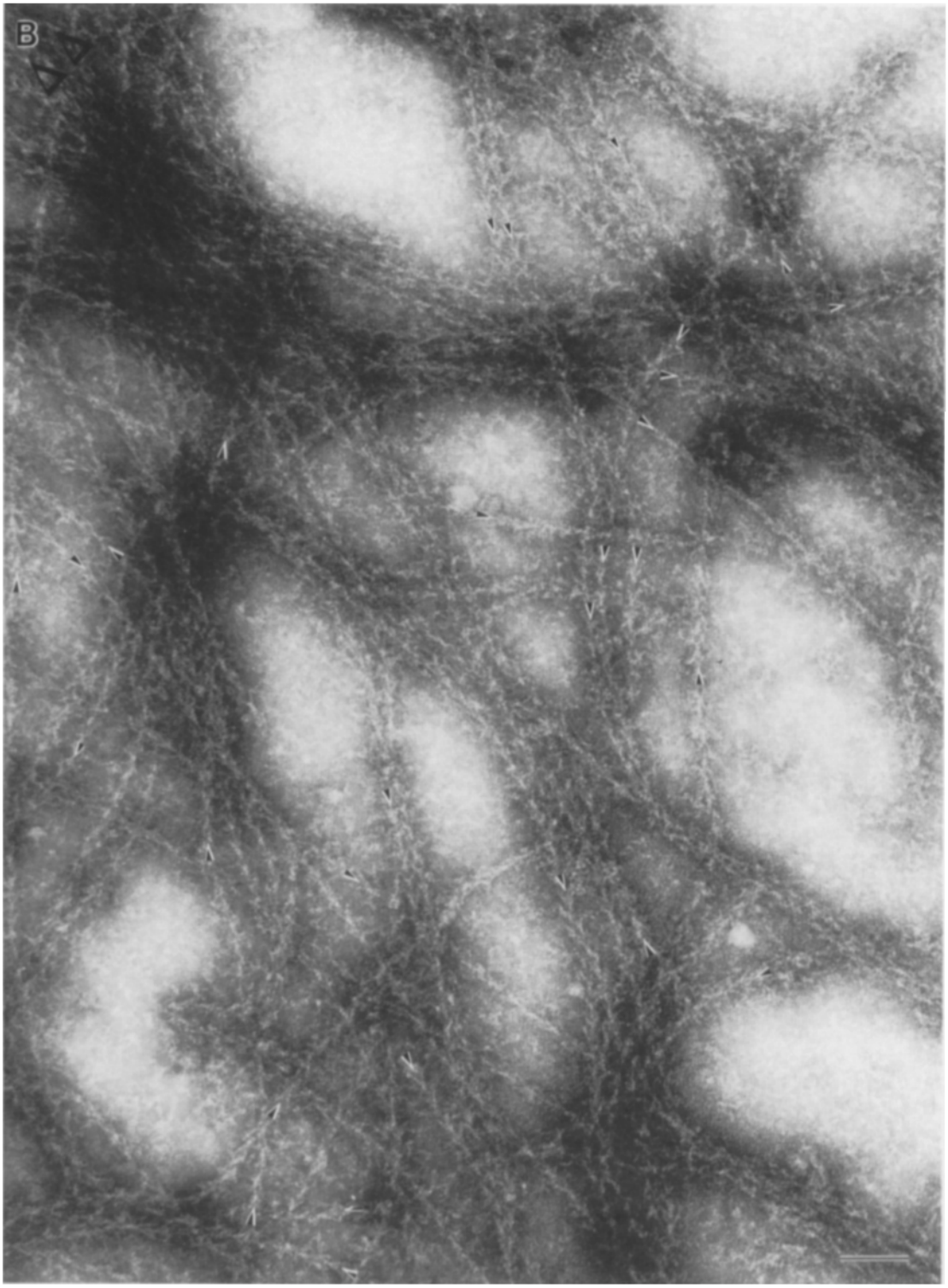

Figure 9.

lipodia appeared to consist of two populations: sheets or bundles of filaments radiating from the leading edge that penetrated through a population of branching filaments that made contacts with the ventral membrane surface and then projected upward. Notably, the contacts that this latter filament population made with the membrane were of two types: direct and indirect. Direct contacts involved bending of the filament as it appeared to touch the membrane surface, so that contact was made along the length of the filament surface, not by filament ends. Indirect contact involved the ends of filaments contacting a second filament that ran parallel to the membrane surface. Often the second filament appeared to be from the long radially oriented bundled filaments.

The second method for physically shearing away the top membrane and filament layer involved sonication of unfixed cells. This generally resulted in stripping away all but a minor population of actin filaments that were in direct contact (lengthwise) with the membrane (Fig. 14). Rarely, filament

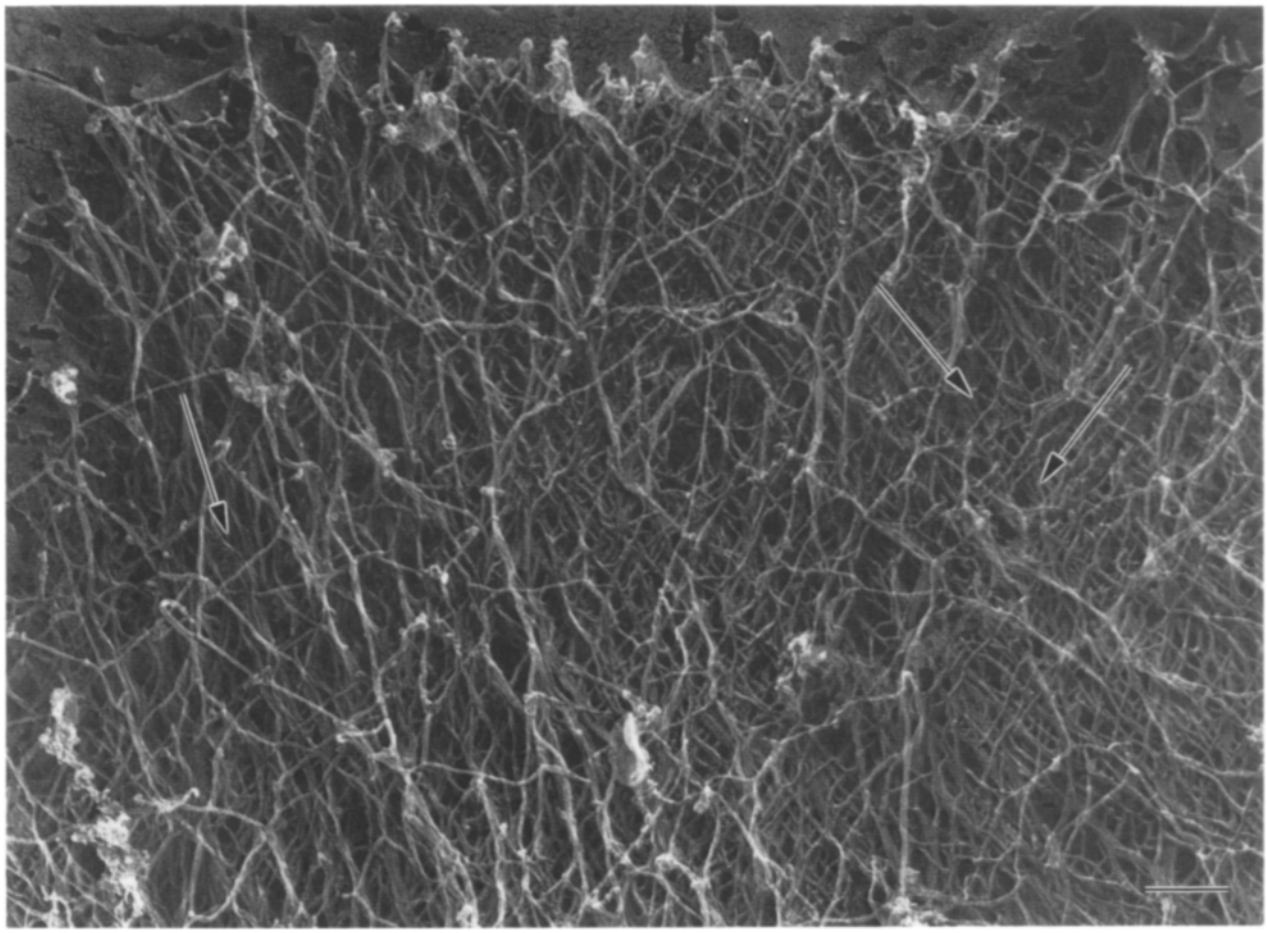

Figure 10. A freeze-etch view of a thin lamellipodium from a growth cone that was saponin permeabilized, fixed, and then Triton-extracted before rapid freezing. The majority of actin filaments radiate from the leading margin, sometimes appearing to interweave as they cross from slightly different angles and levels (*arrows*). Particularly kinked filaments on the surface are apparent; they represent filaments presumably displaced by fluid movement prior to freezing. They sometimes extend beyond the leading margin and appear bright because of the relatively large amount of platinum received during rotary shadowing. Bar, 0.2 μm.

bundles or portions of the meshwork that projected upward could also be seen. In high magnification images, particles on the inner membrane surface appeared to interact with the actin filaments that were retained. In areas of membrane largely devoid of actin filaments, particles were sometimes arranged in rows, suggesting that they had been in contact with actin filaments before the filaments were stripped away by the sonication (Fig. 14 *B*). The predominant orientation of the membrane associated filaments and of the particle rows was perpendicular to the leading edge, similar to that of the actin filaments that radiate from the leading edge back towards the central region of the growth cone.

Freeze Etching of Decorated Samples

In pilot experiments, decorated samples prepared by freeze etching appeared similar to those prepared by negative stain; all actin filaments were obviously decorated when either HMM or S1 were used. However, in contrast to the negative stain images, the polarity of individual decorated filaments was not easily determined without treatment of the sample with tannic acid and uranyl acetate before freezing as described by Heuser (14). Control preparations treated in the same manner showed no detectable change in the organization of actin filaments (data not shown). However, the filament substructure did appear slightly different: in freeze-etch preparations the left handed repeat pattern that is usually seen along the filament was less obvious, while in both freeze-etch and negative stain preparations the filament diameter was slightly increased. These changes are probably associated with binding of the tannic acid and uranyl acetate to the filament. Comparison of HMM and S1 decoration in the freeze etch samples indicated that filament polarity was most easily determined with S1 decoration. Therefore, S1 decoration was used for all subsequent experiments.

In stereo views (Fig. 15), decorated filament arrays appeared to have more depth than those seen in negative stain images. Otherwise the organization appeared very similar: relatively long filaments radiated from the leading edge and intermingled with shorter filaments that were roughly oriented along the z-axis. The only difference seemed to be in the number of free filament ends that could be seen; the decorated preparations seemed to have more free ends than the undecorated. This was only assessed at a qualitative

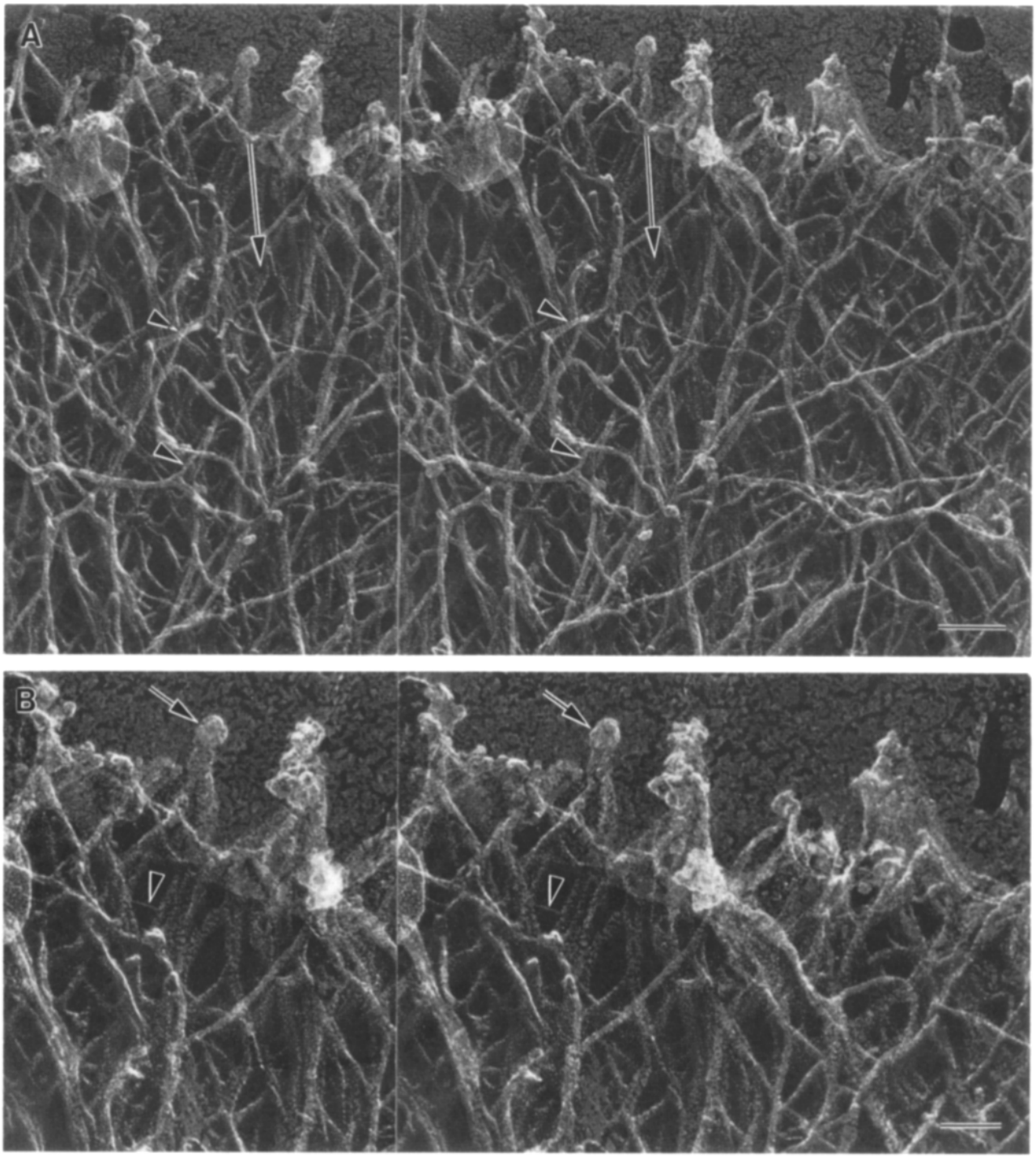

Figure 11. Higher magnification stereo views from the growth cone shown in Fig. 10. (*A*) The general orientation of the longer actin filaments is perpendicular to the leading edge (*large arrows*). A network of shorter filaments orthogonal to the main population is also apparent in the stereo image (*arrowheads*). This population appears to be prominent on the upper surface (they are lighter) while the longer filaments radiating from the leading edge are deeper (appearing darker in the image because of less platinum). (*B*) Many of the filaments radiating from the leading edge appear to have their free ends embedded in a Triton-insoluble globular material (*arrow*). Occasionally short thin filaments bridge two actin filaments (*arrowheads*). Bars: (*A*) 0.1 μm; (*B*) 0.06 μm.

level. As in the negative stain samples, the polarity could be easily determined on some filaments while on others it was difficult to make a positive determination (Figs. 15 and 16). One distinct advantage of the freeze etch images was the ability to determine polarity of filaments in relatively thick regions of the growth cone that were not visible in negative stain images because of the high electron density. However, only the top filament layer could be clearly imaged because deeper filaments did not receive sufficient metal coating. In all images that were obtained, it was clear that the filament

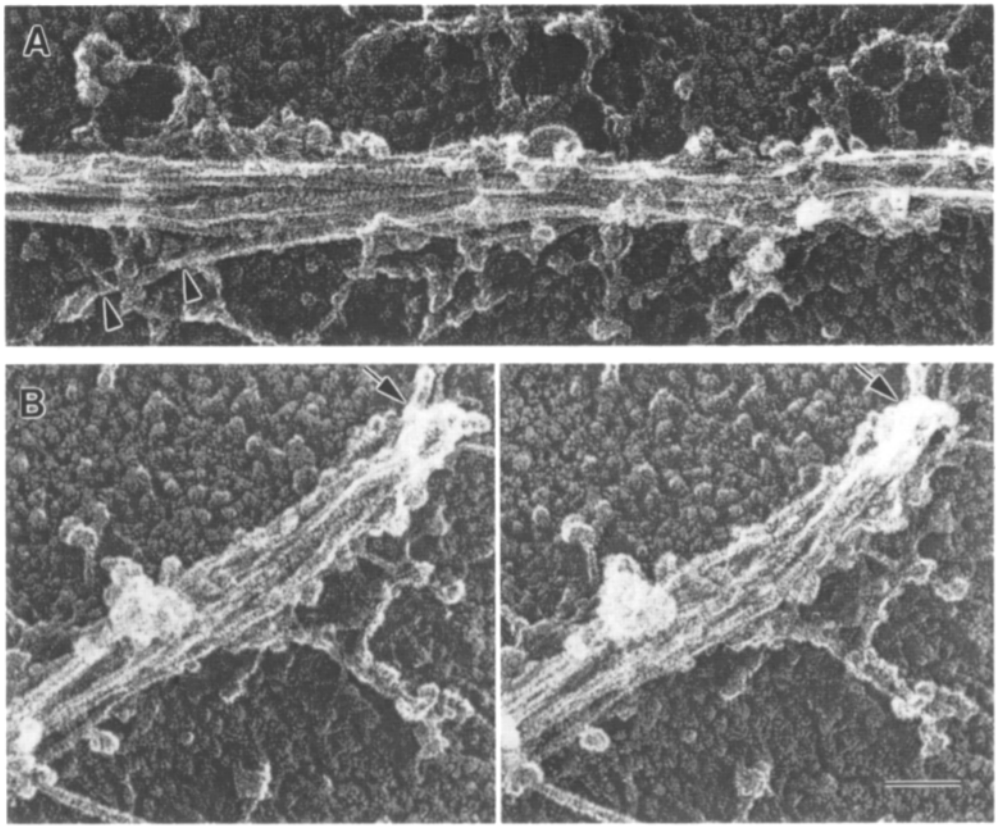

Figure 12. Freeze-etch views of filopodia from growth cones prepared by saponin permeabilization, fixation, and Triton extraction. (*A*) Filaments appear tightly packed, partially due to the increased diameter of the rotary shadowed filaments. The tip of the filopodium is to the left side of the image; one filament can be seen splaying from the main bundle (*arrowheads*). (*B*) Stereo view of a filopodium tip. The free ends of filaments are embedded in a Triton insoluble material (*arrow*). Bar, 0.06 μm.

polarity was not uniform; filaments with completely opposite polarities could be seen and this organization was independent of the particular region of the growth cone.

To obtain a better estimate of filament polarity some simple quantitation was done in a manner similar to that for the negative stain. Quantitation of polarity of the freeze-etched filaments was difficult since it was often not possible to follow a filament for long distances before it intersected other filaments. Usually, because of the metal shadowing, it was not easy to tell whether an intersection was a cross point or a branch point. In general, if a filament emerged on the other side of the intersection with approximately the same course, it was considered a continuation of the same filament. The values obtained were similar to those from the negatively stained samples: the polarity could be determined on 27% of the total filaments within a field, 47% of these had their barbed ends toward the leading edge, 22% with their pointed ends toward the leading edge, and 31% were parallel to the leading edge.

Similar to the negative stain images, the filament bundles that formed the core of filopodia were too tightly packed to accurately distinguish the polarity of the individual filaments. Occasionally, however, individual filaments splayed off from the bundle and it was clear that the filaments had originally extended to or close to the tip of the bundle. In a few such cases filaments were oriented with their pointed end toward the tip of the bundle. However, without further work we cannot rule out the possibility that the filaments were displaced by fluid movement. Also, similar to the negatively stained samples, filaments could be seen entering the base of filopodial bundles with their pointed ends toward the tip.

Discussion

Using both negative stain and freeze–etching techniques in conjunction with a permeabilization protocol that causes little change in growth cone morphology, we have obtained a potentially more accurate and complete picture of the organization of the actin cytoskeleton at the leading edge of neuronal growth cones. This conclusion is based on several factors. First, using high resolution differential interference contrast microscopy, there is little detectable change in overall morphology when growth cones are permeabilized with low concentrations of saponin. Second, at the electron microscopic level, filament density within lamellipodia is high and appears to be more organized (less random) than has been previously shown. After fixation and Triton extraction, changes in filament organization occur, but the views obtained by negative stain or freeze etching closely correspond. Again, this is in contrast to previous reports comparing the two techniques.

The observed organization appears to correlate with the functional state of the leading edge at the time of permeabilization. Functional classifications were based upon observations made of growth cone behavior observed with VEC-DIC microscopy (8, 31). In regions classified as expanding, the predominant feature in the saponin permeabilized negative stain samples are discreet 40–100-nm-wide bundles radiating from the leading edge. The filaments in these bun-

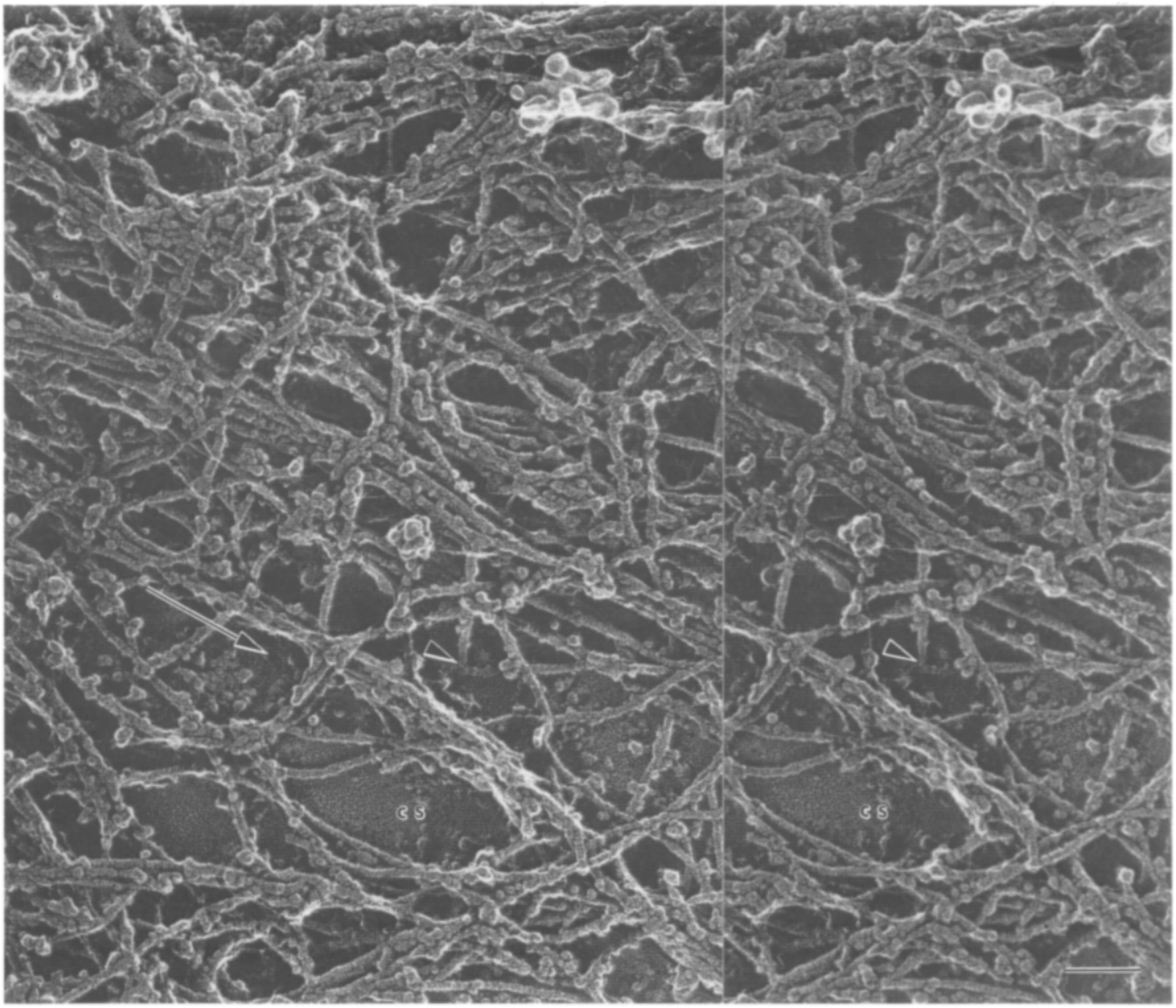

Figure 13. A freeze-etch, stereo view from a growth cone that was prepared by saponin permeabilization, fixation, and then physical shearing just before freezing. Two filament populations can be seen; one is composed of bundled filaments radiating from the leading edge (*large arrow*), while the second intersects the first in an orthogonal orientation, roughly along the z-axis (most obvious in the stereo image). The relationship between actin filaments and the cytoplasmic surface (*cs*) of the ventral membrane can be seen. As filaments approach the membrane surface they either bend and follow it or make contacts with their ends on filaments that appear to lay upon the membrane surface (*arrowhead*). Bar, 0.1 μm.

dles are long (3–6 μm), often extend the entire length of the lamellipodia, and run essentially parallel to each other. The number of filaments in each bundle is variable, but is usually <12. Moreover, the filaments within a bundle appear to be in roughly the same plane. This is in contrast to bundles that form the core of filopodia which have greater numbers of filaments (>15) and contain several layers of filaments. The distal ends of filaments in both types of bundles are closely associated with the leading edge inner membrane surface. The filaments do not appear to directly contact the membrane however, but rather, seem to contact an amorphous or globular material closely associated with the membrane surface. These bundles penetrate through a second population of randomly oriented filaments that fill the volume between the top and bottom membrane surfaces. This second population of filaments is made up of shorter filaments that branch or cross extensively. These filaments are also seen in areas of the leading edge that are either stationary or retracting, while the radially oriented bundles are not seen in these areas.

Triton extraction after the samples have been fixed removes the membrane completely, yet appears to leave the actin cytoskeleton reasonably intact, with some changes in organization. Samples that have been Triton extracted after fixation do not have the small bundles, but rather, long actin filaments splay out from the leading edge as individual filaments that run at oblique angles from each other. The 40–100-nm-wide bundles in the saponin samples and the splaying filaments in the Triton-extracted samples probably represent the same filament population. This suggests that

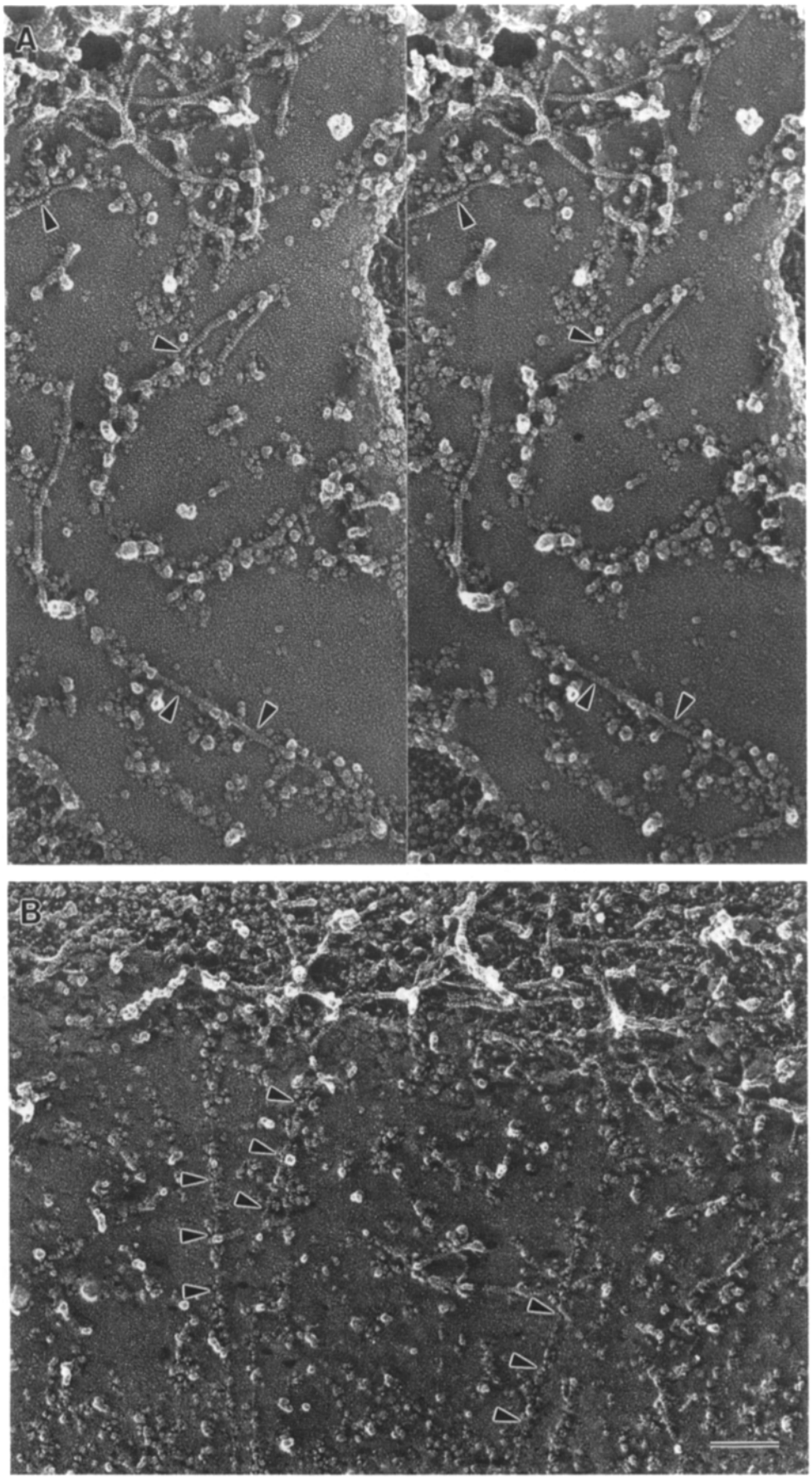

Figure 14. Freeze-etch views from growth cones sheared open by sonication and then fixed before freezing. (*A*) In the stereo image the relationship between the few remaining actin filaments and particles on the inner membrane surface can be seen. The leading edge is towards the top of the image. Individual actin filaments appear to directly contact the particles (*arrowheads*). (*B*) From a growth cone in which most of the actin filaments were sheared away by the sonication. Membrane associated particles form tracks (*arrowheads*) perpendicular to leading edge. Bar, 0.1 μm.

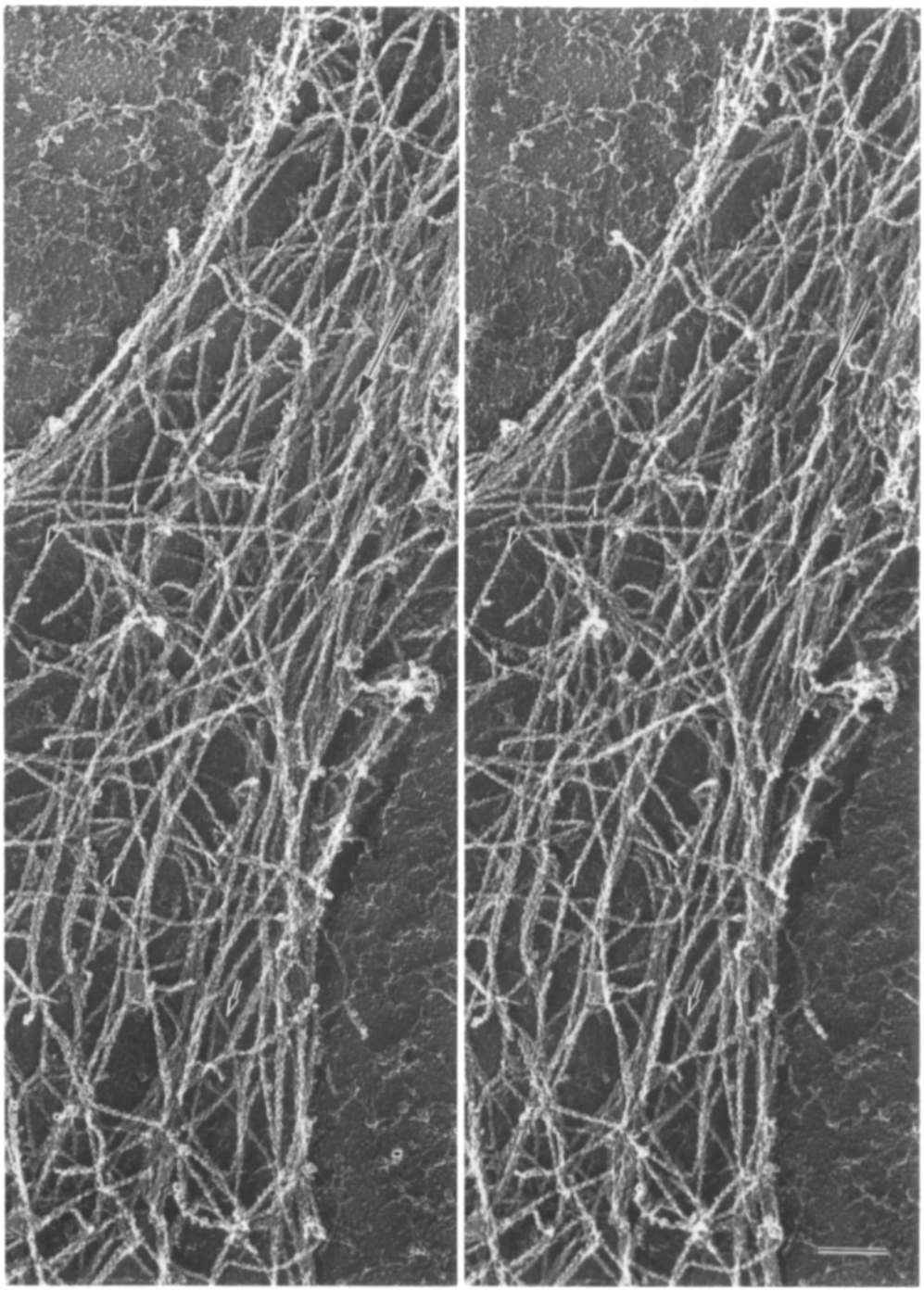

Figure 15. Stereo view of a portion of a growth cone that was permeabilized with saponin, decorated with S1, fixed/Triton extracted and then freeze etched, rotary shadowed. The polarity of the filaments (*arrowheads*) can be clearly seen on many of the filaments. Long filaments extend roughly perpendicular to the leading edge (direction indicated by *long arrow*; leading edge toward top right corner) and weave through a shorter filament meshwork, similar to the organization observed in the negative stain images, although the freeze-etch images show considerably more depth. Short arrow indicates example of a meshwork filament extending along the z-axis. Bar, 0.3 μm.

the presence of the membrane is required to keep the filaments bundled and its removal leads to loss of the bundle organization and a transformation into individual splaying filaments. However, we cannot rule out the possibility that the bundles are removed with the membrane upon Triton extraction and the long splaying filaments represent another filament subset.

It is interesting that the interaction of actin filaments with the ventral membrane surface appears to occur only along the length of individual filaments and not through association of the filament tips with the membrane. This is true for both the long, bundled, radially oriented filaments and the short filaments that fill the volume between the two membrane surfaces: upon approaching the membrane they either bend and run parallel to the surface or their tips contact a second filament running roughly in an orthogonal direction along the membrane surface. The observation that fairly long and straight membrane particle tracks oriented perpendicular to the leading edge are present postsonication further supports the idea that the filaments associate with the membrane and/or membrane-associated proteins along their length. These membrane-associated filaments may be displaced or removed when cells are extracted with Triton. It may be significant that the only area where interaction between fila-

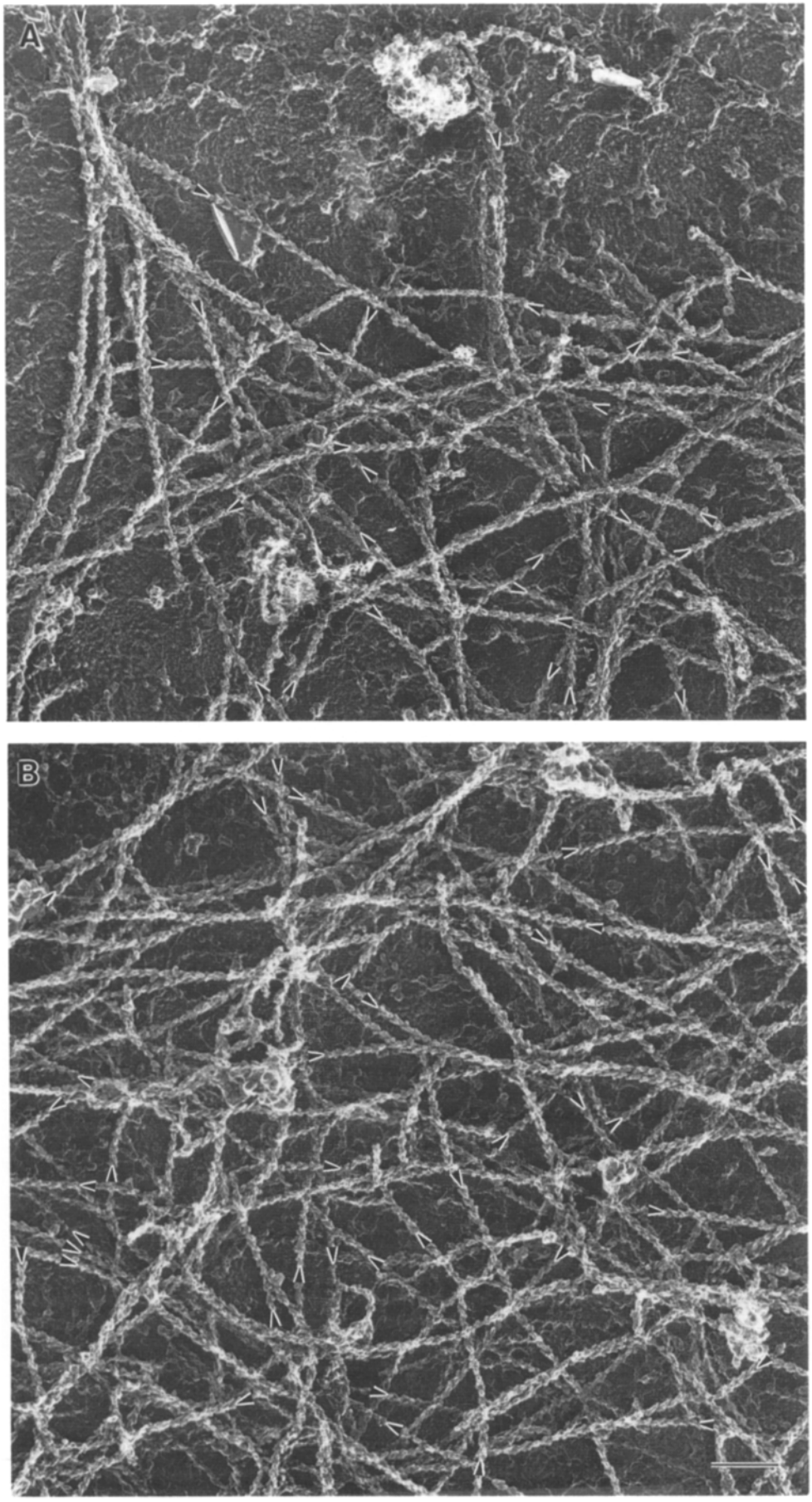

Figure 16. High magnification images of a growth cone prepared as described for Fig. 15. Comparison of the leading edge (*A*) and region slightly further back (*B*). Again the polarity of the filaments (*arrowheads*) is mixed, although the predominant orientation is with the barbed end pointed towards the leading edge. Leading edge is toward the top (*A* and *B*). Bar, 0.2 μm.

ment free ends and the membrane surface is observed is at the leading edge, where free ends of actin filaments appear to be associated with a Triton-insoluble globular material. A similar material has also been seen in fibroblasts (39). The identity of this material is not known but could represent a barbed-end capping protein or other actin binding protein involved in regulating the rate of filament polymerization (10). This observation is consistent with the idea that actin polymerization at the leading edge is coupled to cell motility and that the polymerization is tightly regulated by actin binding proteins.

Orientation with Respect to Polarity

Previous reports of actin filament polarity have suggested that filament polarity in lamellipodia and filopodia in various cell types is uniform (1, 19, 36), with the barbed, or rapidly polymerizing, ends of the filaments directed exclusively toward the leading edge or filopodial tip. In contrast to these previous results, in neuronal growth cones we never observed uniform filament polarity.

The discrepancy between our results and previous polarity studies could be attributed to several factors. First, the differences in decoration protocols: in this study decoration was done after permeabilization with a low concentration of saponin, while previous studies used extraction with Triton or glycerol prior to decoration. We have demonstrated that the permeabilization protocol using saponin is optimal for preserving the overall morphology of the growth cone cytoskeleton. Second, we analyzed the polarity of many filaments within a field in several regions of the lamellipodia, not simply a few filaments at the extreme edge as has been done in some previous studies (19, 36). Third, growth cones may have an intrinsically different actin filament arrangement than that found in nonneuronal cells or in neuroblastoma cells (38). While any one or all of these possibilities could contribute to the difference in results, we feel that the first two are the most likely to be important.

The polarity of individual actin filaments may correspond to their identity with one of the two distinct filament populations. We observed that although the polarity of actin filaments in growth cone lamellipodia was not uniform, there was a predominant orientation with 47–55% of the filaments oriented with their barbed ends toward the leading edge. The population of long filaments radiating from the leading edge, associated in small 40–100-nm-wide bundles, may be oriented primarily (but not exclusively) with their barbed ends directed toward the leading edge. The second population, composed of a meshwork of shorter filaments filling the volume between the dorsal and ventral membranes appears to have a random polarity. Superimposition of these two populations into a two-dimensional image would give a result such as the one that we observed: a mixed polarity with a predominant orientation in relation to the leading edge. Unfortunately, it was difficult to precisely determine the relationship between filament polarity and population since the distinction between the two filament populations was not as readily apparent in the decorated, and simultaneously fixed and Triton-extracted growth cones. However, our observations and quantitation of the decorated filaments supports this hypothesis and our interpretation of the data is summarized in Fig. 17.

Previous models of cell motility and the role of the actin cytoskeleton in association with myosin motors and other actin binding proteins have been based on the assumption that the polarity of the filaments is uniform. While our results do not negate these motility models, it is clear that the nonuniform polarity of the lamellipodial and possibly filopodial actin filaments needs to be taken into account.

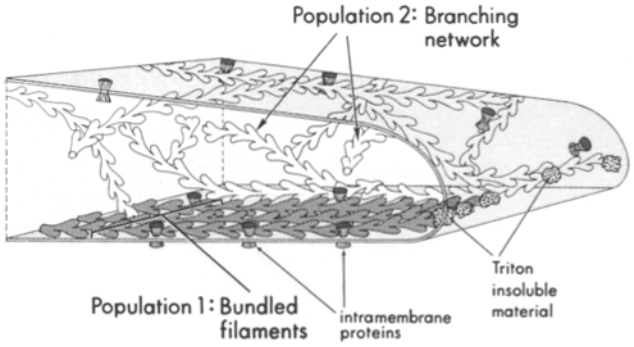

Figure 17. A diagram summarizing the organization and polarity of actin filaments within lamellipodia. The filaments organized in small bundles that radiate from the leading edge are shown in black while the short, branching meshwork of filaments are indicated in white. All filaments are shown decorated with myosin subfragments to indicate polarity. The polarity of the entire complement of filaments is mixed because the meshwork (white) filaments have a random orientation. Barbed end tips of filaments at the leading edge interact with a globular material that presumably represents a cytoplasmic protein. Integral membrane proteins are also shown; their possible arrangement and association with filaments is indicated.

The mixed polarity we observe is at least partially consistent with the nucleation release model of Theriot and Mitchison (42). This model predicts a randomly oriented population of relatively short filaments uniformly distributed throughout the lamellae. Apparently, this model is not fully consistent with our data because two populations of filaments are present instead of a single population described by the model. The randomly oriented population of short filaments that we detect may be similar to the population described by the model.

Functional Roles of the Two Filament Populations

The two filament populations may have distinct functions. The long radially oriented bundles could be involved in expansion of the leading edge. Their polarity and presence within regions that can be classified as expanding is consistent with this conclusion. Since they also appear to be primarily (although possibly not exclusively) associated with the ventral membrane surface, they may also be involved in the interaction with the substrate. Filaments along the ventral surface appear to interact with membrane-associated particles that could represent integral membrane proteins. If these proteins are receptors for substrate proteins such as laminin, a mechanism coupling the actin filaments to the substrate via these receptor proteins can be envisioned. Both populations probably have some role in membrane–substrate interactions, but the more ventral location of the long radially oriented filaments suggests that they may have a primary role in such interactions. The shorter meshwork filaments may act as scaffolding, maintaining the volume of the lamellipodia. They may also be the primary component of the

retrograde flow of actin filaments that is readily apparent with differential interference contrast microscopy (13).

In addition, the differences in filament length and organization (bundled versus meshwork) of the two filament populations suggest that they may differ in stability. In vitro, long actin filaments are more stable than shorter filaments (10), suggesting that in vivo the long bundled filaments may represent a more stable population of filaments than the shorter filaments of the meshwork. Their orientation and relatively long length also suggests that this population may be likely to exhibit treadmilling of monomers during locomotion. It is interesting that this potentially more stable population of filaments may also be primarily involved in associations with membrane proteins that could mediate interactions with the substratum.

Using photoactivatable fluorescently labeled actin monomers, Theriot and Mitchison (42) have recently demonstrated that, in fish keratocytes, a population of actin filaments is present in lamellae that appear to be stationary relative to the substratum during rapid movement. This is in contrast to studies which have demonstrated a population of actin filaments in lamellae that show a retrograde flow indicative of treadmilling (43), or a faster bulk retrograde flow of filaments (12, 13) in slow moving or stationary cells. These conflicting observations would be reconciled if the different techniques that have been used preferentially labeled filament populations that differ in stability, mobility, and their manner of coupling to proteins that mediate interaction with the substratum during locomotion. A similar conclusion has been reached by others (22). Our observations are consistent with this interpretation and provide structural evidence for two distinct populations of filaments. The interaction between these two filament populations may represent the basis for the complex behavior observed within lamellipodia, which includes protrusion at the leading edge, bulk retrograde movement of actin filaments, ruffling or waving movements of lamellipodia and filopodia and the generation of tension through interaction with membrane receptors for substrate molecules. It will be difficult to further speculate on the molecular interactions that underlie these phenomena until more precise information is available on the exact location of other important proteins, such as the myosins, that are likely to be involved in these processes. For instance, depending on the location and type of myosin present relative to these two populations of actin filaments, different behaviors will result. It will therefore be important in future work to clearly demonstrate the relationship between myosin type and its location relative to these two actin filament populations.

We thank Grady Phillips for technical assistance, Charles Ross for polarity identification, and John Cooper, Elliot Elson, and Bill Rochlin for reading the manuscript.

This work was supported by grants NS26150 and NS15070 to P. C. Bridgman.

Received for publication 7 February 1992 and in revised form 5 August 1992.

References

1. Begg, D. A., R. Rodewald, and L. I. Rebhun. 1978. The visualization of actin filament polarity in thin sections: evidence of the uniform polarity of membrane-associated filaments. *J. Cell Biol.* 79:846–852.
2. Bottenstein, J. E., and G. H. Sato. 1979. Growth of rat neuroblastoma cell-line in serum-free supplemented medium. *Proc. Natl. Acad. Sci. USA.* 76(1):514–517.
3. Bridgman, P. C., and M. E. Dailey. 1989. The organization of myosin and actin in rapid frozen nerve growth cones. *J. Cell Biol.* 108:95–109.
4. Bridgman, P. C., and Y. Nakajima. 1983. Distribution of filipin-sterol complexes on cultured muscle cells: cell-substratum contact areas associated with acetylcholine receptor clusters. *J. Cell Biol.* 96:363–372.
5. Bridgman, P. C., and T. S. Reese. 1984. The structure of cytoplasm in directly frozen cultured cells. 1. Filamentous meshworks and the cytoplasmic ground substance. *J. Cell Biol.* 99:1655–1668.
6. Bridgman, P. C., C. Carr, S. E. Pederson, and J. B. Cohen. 1987. Visualization of the cytoplasmic surface of torpedo postsynaptic membranes by freeze-etch and immunoelectron microscopy. *J. Cell Biol.* 105: 1829–1846.
7. Bridgman, P. C., A. K. Lewis, and J. C. Victor. 1992. Comparison of the ability of freeze-etch and freeze-substitution to preserve actin filament structure. *J. Elect. Microscope Tech.* In press.
8. Burmeister, D. W., M. Chen, C. H. Bailey, and D. J. Goldberg. 1988. The Distribution and movement of organelles in maturing growth cones: correlated video-enhanced and electron microscopic studies. *J. Neurocyt.* 17:783–795.
9. Caldwell, P. C. 1970. Calcium chelation and buffers. *In* Calcium and Cellular Function. A. W. Cuthbert, editor. MacMillan, London. 10–16.
10. Cooper, J. A. 1991. The role of actin polymerization in cell motility. *Annu. Rev. Physiol.* 53:585–605.
11. Dailey, M. E., and P. C. Bridgman. 1991. Structure and organization of membrane organelles along distal microtubule segments in growth cones. *J. Neurosci. Res.* 30:242–258.
12. DeBiasio, R. L., L-L. Wang, G. W. Fisher, and D. L. Taylor. 1988. The dynamic distribution of fluorescent analogues of actin and myosin in protrusions at the leading edge of migrating Swiss 3T3 fibroblasts. *J. Cell Biol.* 107:2631–2645.
13. Forscher, P., and S. J. Smith. 1988. Actions of cytochalasins on the organization of actin filaments and microtubules in a neuronal growth cone. *J. Cell Biol.* 107:1505–1516.
14. Heuser, J. E. 1983. Structure of the myosin crossbridge lattice in insect flight muscle. *J. Mol. Biol.* 169:123–154.
15. Heuser, J. E., and R. G. W. Anderson. 1989. Hypertonic media inhibit receptor-mediated endocytosis by blocking clathrin-coated pit formation. *J. Cell Biol.* 108:389–400.
16. Heuser, J. E., and M. W. Kirschner. 1980. Filament organization revealed in platinum replicas of freeze-dried cytoskeletons. *J. Cell Biol.* 86: 212–234.
17. Hirokawa, N., L. G. Tilney, K. Fujiwara, and J. E. Heuser. 1982. Organization of actin, myosin, and intermediate filaments in the brush border of intestinal epithelial cells. *J. Cell Biol.* 94:425–443.
18. Huxley, H. E. 1963. Electron microscope studies on the structure of natural and synthetic protein filaments from striated muscle. *J. Mol. Biol.* 7:281–308.
19. Isenberg, G., and J. V. Small. 1978. Filamentous actin, 100 A filaments and microtubules in neuroblastoma cells. Their distribution in relation to sites of movement and neuronal transport. *Cytobiologie.* 16:326–344.
20. Johnson, M. I., and V. Argiro. 1983. Techniques in the tissue culture of rat sympathetic neurons. *Methods Enzym.* 103:334–347.
21. Kielley, W. W., and W. F. Harrington. 1960. A model for the myosin molecule. *Bioc. Biop. Acta.* 41:401.
22. Kucik, D. F., E. L. Elson, and Y. L. Wang. 1991. Actin tracks. *Nature (Lond.).* 354:362–363.
23. Kuczmarski, E. R., and J. L. Rosenbaum. 1979. Studies of the organization and localization of actin and myosin in neurons. *J. Cell Biol.* 80:356–371.
24. Letourneau, P. C., and A. H. Ressler. 1983. Differences in the organization of actin in the growth cones compared with the neurites of cultured neurons from chick embryos. *J. Cell Biol.* 97:963–973.
25. Lowey, S., and S. S. Margossian. 1982. Preparation of myosin and its subfragments from rabbit skeletal muscle. *Methods Enzymol.* 85:55–71.
26. Maupin, P., and T. D. Pollard. 1983. Improved preservation and staining of HeLa cell actin filaments, clathrin-coated membranes, and other cytoplasmic structures by tannic acid-glutaraldehyde-saponin fixation. *J. Cell Biol.* 96:51–62.
27. Mitchison, T., and M. Kirschner. 1988. Cytoskeletal dynamics and nerve growth. *Neuron.* 1:761–772.
28. Moore, P. B., H. E. Huxley, and D. J. DeRosier. 1970. Three-dimensional reconstruction of F-actin, thin filaments and decorated thin filaments. *J. Mol. Biol.* 50:279–295.
29. Pollard, T. D., S. K. Doberstein, and H. G. Zot. 1991. Myosin-I. *Annu. Rev. Physiol.* 53:653–681.
30. Rees, R. P., and T. S. Reese. 1981. New structural features of freeze-substituted neuritic growth cones. *Neuroscience.* 6:247–254.
31. Rinnerthaler, G., M. Herzog, M. Klappacher, H. Kunka, and J. V. Small. 1991. Leading edge movement and ultrastructure in mouse macrophages. *J. Struct. Biol.* 106:1–16.
32. Ris, H. 1985. The cytoplasmic filament system in critical point-dried whole mounts and plastic-embedded sections. *J. Cell Biol.* 100:1474–1487.
33. Ryder, M. I., R. N. Weinrab, and R. Niederman. 1984. The organization

of actin filaments in human polymorphonuclear leukocytes. *Anat. Rec.* 209:7–20.
34. Sellers, J. R., and B. Kachar. 1990. Polarity and velocity of sliding filaments: control of direction by actin and of speed by myosin. *Science* 249:406–408.
35. Small, J. V. 1988. The actin cytoskeleton. *Electron Microsc. Rev.* 1:155–174.
36. Small, J. V., and J. E. Celis. 1978. Filament arrangements in negatively stained cultured cells: the organization of actin. *Cytobiologie.* 16:308–325.
37. Small, J. V., and G. Langanger. 1981. Organization of actin in the leading edge of cultured cells: influence of osmium tetroxide and dehydration on the ultrastructure of actin meshworks. *J. Cell Biol.* 91:695–705.
38. Small, J. V., G. Isenberg, and J. E. Celis. 1978. Polarity of actin at the leading edge of cultured cells. *Nature (Lond.).* 272:638–639.
39. Small, J. V., G. Rinnerthaler, and H. Hinssen. 1982. Organization of actin meshworks in cultured cells: the leading edge. *Cold Spring Harbor Symp.* 46:599–611.
40. Smith, S. J. 1988. Neuronal cytomechanics: the actin-based motility of growth cones. *Science (Wash. DC).* 242:708–715.
41. Stossel, T. P. 1984. Contribution of actin to the structure of the cytoplasmic matrix. *J. Cell Biol.* 99(1):15s–21s.
42. Theriot, J. A., and T. Mitchison. 1991. Actin microfilament dynamics in locomoting cells. *Nature (Lond.).* 352:126–131.
43. Wang, Y. L. 1985. Exchange of actin subunits at the leading edge of living fibroblasts: possible role of treadmilling. *J. Cell Biol.* 101:597–602.
44. Wolosewick, J. J., and K. R. Porter. 1979. Microtrabecular lattice of the cytoplasmic ground substance: artifact or reality. *J. Cell Biol.* 82:114–139.
45. Yamada, K. M., B. S. Spooner, and N. K. Wessells. 1971. Ultrastructure and Function of Growth Cones and Axons of Cultured Nerve Cells. *J. Cell Biol.* 49:614–635.